

HU/CC 76-1 / TR-189
AD NO. 27-718

ASTIA FILE COPY

Office of Naval Research

Contract N50RI-76 • Task Order No.1 • NR-020-011

RELAXATION EFFECTS IN PARAMAGNETIC AND
FERROMAGNETIC RESONANCE

28



PROPERTY OF R.D:
TECHNICAL LIBRARY

By

N. Bloembergen and S. Wang

September 10, 1953

Technical Report No. 188

Cruft Laboratory
Harvard University
Cambridge, Massachusetts

Office of Naval Research

Contract N5-ori-76

Task Order No. 1

NR-078-011

Technical Report

on

Relaxation Effects in Paramagnetic and Ferromagnetic Resonance

by

N. Bloembergen and S. Wang

September 10, 1953

The research reported in this document was made possible through support extended Cruft Laboratory, Harvard University, jointly by the Navy Department (Office of Naval Research), the Signal Corps of the U. S. Army, and the U. S. Air Force, under ONR Contract N5ori-76, T. O. 1.

Technical Report No. 188

Cruft Laboratory

Harvard University

Cambridge, Massachusetts

TR188

Relaxation Effects in Paramagnetic and Ferromagnetic Resonance

N. Bloembergen and S. Wang

Division of Applied Science, Harvard University

Cambridge, Massachusetts

Abstract

Magnetic resonance experiments have been carried out at 3 cm wavelength in paramagnetic and ferromagnetic samples at very high microwave power levels, in a temperature range between 77°K and 700°K. Changes in the microwave susceptibility and the d-c magnetization have been observed for microwave amplitudes between 1 and 50 oersted.

For a paramagnetic salt, $MnSO_4 \cdot 4H_2O$, these changes are readily interpreted in terms of a spin-lattice relaxation mechanism. The value for the spin-lattice relaxation time is derived in three different ways and agrees well with that obtained by Gorter's non-resonant method.

When a large exchange interaction occurs between the spins, the situation above the Curie point can be described in terms of a conversion of magnetic into exchange energy. The magnetic and the spin-exchange systems are not always in thermal equilibrium. The characteristic time for the transfer of energy between these systems is equal to the inverse of the line width, which is given by the Van Vleck-Anderson formula for exchange narrowing. Experimental results for an organic free radical and some ferrites confirm this point of view.

Below the Curie temperature the situation is more complicated. The experimental data for several ferrites and supermalloy show qualitatively the same behavior.

The absorbed magnetic energy is again converted into exchange energy with a characteristic time which is always shorter than 3×10^{-8} sec. At high temperatures this time is equal to the inverse line width and the transition to the paramagnetic region is continuous. At low temperatures the relaxation time increases roughly inversely proportional to the temperature, although the width remains constant. The microwave susceptibility has an anomalous decrease at high power levels. These effects have found no satisfactory explanation in existing theories.

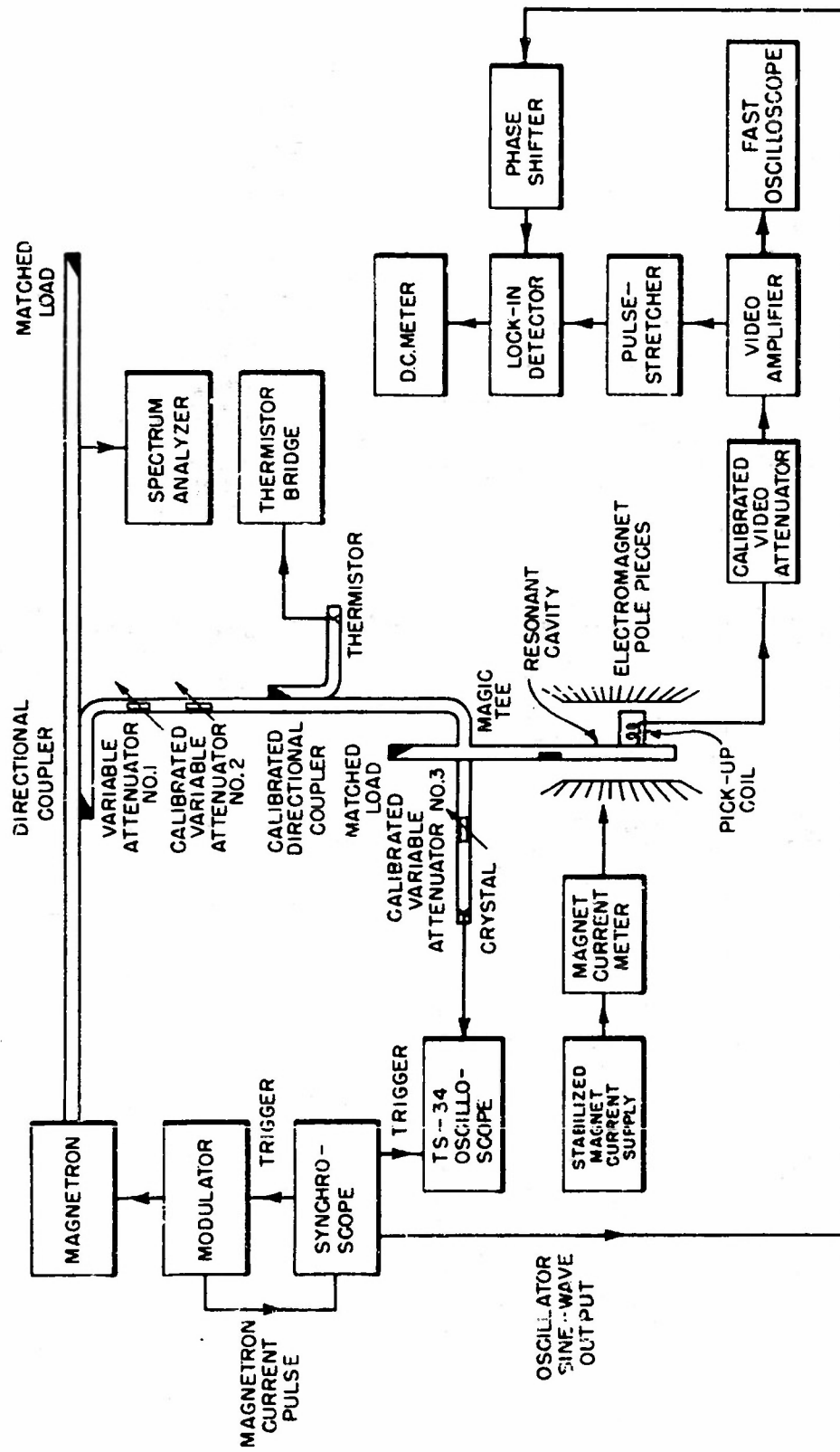
-I-

The Experimental Method and Its Application to a Paramagnetic Salt

Numerous investigations have been made of spin-spin relaxation and spin-lattice relaxation in both electronic and nuclear paramagnetism. Gorter and co-workers originally investigated relaxation times in paramagnetic salts by non-resonant methods.¹

The determination of relaxation times by resonance methods was first carried out for nuclear spin systems² and subsequently applied to electron spins by Slichter.³ This so-called saturation method has been extended and improved. For the first time the z-component of the magnetization at resonance is observed.⁴ A detailed description of the method has recently been given by Damon.⁵ We shall here only mention its most important features and some recent improvements.

Microwave power from a pulsed tunable 2J51 magnetron excites a cavity, through an inductive iris. The cavity is a shorted X-band guide, $2\lambda_g$ long. With the aid of calibrated attenuators the amplitude of the microwave field can be varied up to 50 gauss. This value corresponds to 15000 volts/cm which is near dielectric breakdown in the cavity. The magnetic sample is placed one guide wavelength from the end wall near a slit milled in the center of the broad side of the guide, 0.4 cm wide and $\frac{1}{2}\lambda_g$ long. The presence of the slit did not lower the Q of the cavity more than 10%. No thin metallized window with choke coupling was needed as in the earlier arrangement.⁵ A pick-up coil consisting of 10 turns, 1 cm in diameter, is placed near the slit outside the cavity. The d-c magnetic field H_0 is perpendicular to the broad side of the cavity and parallel to the axis of the pick-up coil. The coil is connected by a coaxial line to a pulse amplifier, the output of which can be displayed on a fast oscilloscope. The pulse amplitude can alternatively be read on the output meter of a detector system described by Damon. Any variations in the d-c magnetization of the sample can thus be recorded. These will occur only at sufficiently high microwave power level when the magnetization swings away from the direction of H_0 . Typical signals are shown in Figures 2 and 3. The voltage induced in the pick-up coil is proportional to dM_z/dt .



BLOCK DIAGRAM OF EQUIPMENT

Fig. 1. Schematic circuit diagram for the measurement of microwave susceptibility and the z-component of magnetization, as a function of the microwave amplitude.

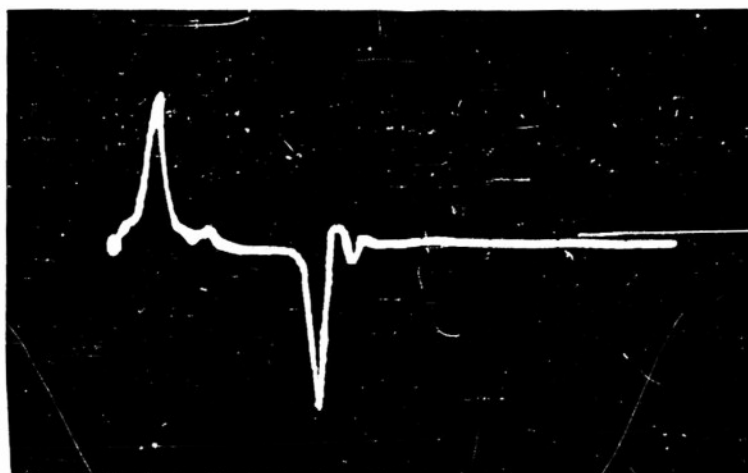


Fig. 2. The induced signal by the change in d-c-magnetization. Two spikes with opposite sign occur at the leading and the trailing edge of the magnetron pulse, corresponding respectively to a decrease and a restoration of the magnetization. The magnitude of the pulses depends on the microwave power level. The decay constant of the pulses is 1.5×10^{-7} sec and is determined by the time constants of the apparatus. Such a pattern is obtained for all samples, if the relaxation time is shorter than 10^{-7} sec.

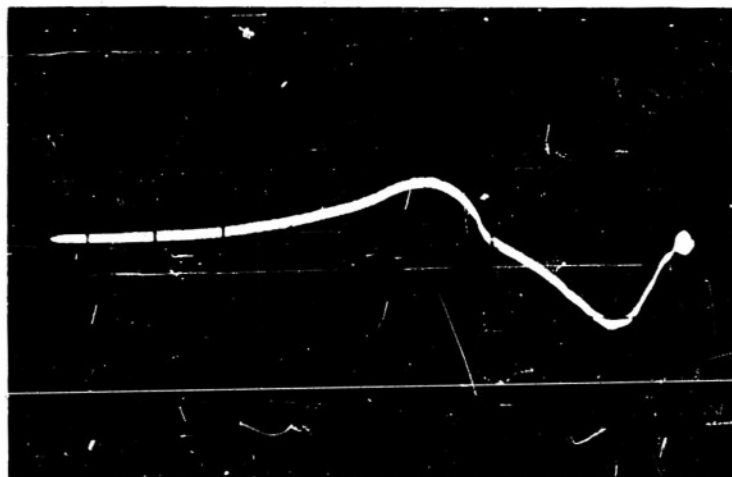


Fig. 3. The induced signal by the change in d-c-magnetization of saturated $\text{MnSO}_4 \cdot \text{H}_2\text{O}$ at 77°K . The decay constant of the trailing pulse is determined by the spin-lattice relaxation time and amounts to 1.2×10^{-6} sec. The decay of the leading pulse is somewhat faster, depending on the incident microwave power.

At the end of the magnetron pulse the magnetization returns to its equilibrium value M_0 according to

$$M_z = (M_z - M_0) e^{-t/\tau} + M_0$$

The time τ is either the ringing time of the microwave power in the cavity or the magnetic relaxation time, whichever is longer. The current induced in the pick-up coil with self-inductance L and input resistance of the pulse amplifier R is given by

$$L \frac{di}{dt} + R i = A \frac{dM_z}{dt}$$

A is a geometric factor depending upon the positions of sample and coil. Substituting M_z from the first equation into the second, we obtain a solution for the induced current

$$i = A(M_z - M_0) (L - R\tau)^{-1} \left[e^{-t/\tau} - e^{-Rt/L} \right]$$

The induced current at the end of the pulse consists of two exponential components and reaches a maximum value of

$$i_{\max} = \frac{A}{L} (M_0 - M_z) \left(\frac{L}{R\tau} \right) \frac{R\tau}{R\tau - L}$$

The maximum deflection is directly proportional to $M_z - M_0$. In order to compare data at different temperatures when both the ringing time and the relaxation time and consequently τ may have changed, the last factor involving τ should be taken into account.

A similar relationship exists at the onset of the magnetron pulse when the magnetization tends to a new equilibrium value smaller than M_0 . It is seen that a steady state is reached during the one microsecond pulse in the recording of Figure 2. The decay in this case is determined by a characteristic time of the apparatus. It is not the ringing of the cavity which is 2×10^{-8} sec for $Q = 2500$ nor the response time of the pick-up coil which is 8×10^{-8} sec, but is mainly due to the rise time of the magnetron power, which is 1.5×10^{-7} sec. The relaxation time of the magnetic spins must be shorter than this time. This situation holds in all samples investigated with one exception, $MnSO_4 \cdot 4H_2O$ at $77^\circ K$. This salt gave the oscillogram of Figure 3. The decay is much slower and the initial pulse

of the leading edge has not decayed completely after one microsecond when the microwave power is shut off. The characteristic time, which must be identified with the spin-lattice relaxation time in this case, is 1.2×10^{-6} sec. Besides this method of direct observation of the M_z decay, there is fortunately another way for determining the relaxation time from the maximum pulse deflection, which is applicable even when the relaxation time is shorter than the response time of the apparatus. When $M_z - M_0$ is plotted as a function of the microwave amplitude a value of the relaxation time can be obtained as will be outlined below.

A third, more familiar, method consists of the determination of the microwave susceptibility and plotting the imaginary part versus the microwave amplitude. This quantity can be calculated from the observed changes in the reflection coefficient of the cavity when magnetic resonance occurs.

A fourth method, which has not been applied here, would be provided by the direct observation of the recovery of the value of χ'' in a small microwave field, immediately after the large microwave field from the magnetron has been taken off.

A complete description of the magnetization would require the knowledge of two independent complex components of the antisymmetric susceptibility tensor^{6,7,8,9} besides the static z-component. When a rectangular cavity is used, the data can be interpreted in terms of one complex scalar susceptibility,

$$\chi' - i\chi'' = (\mu' - i\mu'' - 1)/4\pi = M_x/H_1 \quad (1)$$

The y-component of the microwave field is suppressed by the shorted guide, the corresponding modes being beyond cut-off. The observed change in cavity Q gives the imaginary part of this scalar susceptibility. The change in resonant frequency of the cavity would give the real part, which can also be calculated from the imaginary part with the aid of the Kramers-Kronig relation, which hold for the individual tensor components.⁹ During our experiments the magnetron was always retuned to the cavity resonance. The required frequency changes have not been measured, as they would be much more inaccurate than the determination of Q. At the center of the magnetic resonance χ' is zero. The y-component of the magnetization remains

unobserved in our experiment, but is related to the x-component from equations in a simple fashion.¹⁰

We shall now describe the results when the method is applied to a paramagnetic salt, $MnSO_4 \cdot 4H_2O$. Since the theory for relaxation in paramagnetic media is well understood and since data for the relaxation time in this salt have also been determined by the non-resonant dispersion, this will serve as a check on the reliability of the experimental method. It has been well established that in paramagnetic media without exchange the magnetic resonance and relaxation can be described by the Bloch equations

$$\begin{aligned} \frac{dM_{x,y}}{dt} &= \gamma (M \times H)_{x,y} - \frac{M_{x,y}}{T_2} \\ \frac{dM_z}{dt} &= \gamma (M \times H)_z - \frac{M_z - M_0}{T_1} \end{aligned} \quad (2)$$

In our experiment the magnetic field H has the components

$$H_x = H_1 e^{i\omega t}$$

$$H_y = 0$$

$$H_z = H_0$$

The steady state solution of the set of equations (2) leads to the following value of the observed quantities, the z-component magnetization and the imaginary part of the susceptibility,

$$\chi'' = \mu''/4\pi = \frac{8\pi\omega T_2 \gamma^2 H_0 M_0}{4\omega^2 + T_2^2(\omega_0^2 - \omega^2 + T_2^{-2})^2 + \frac{1}{2}\gamma^2 H_1^2 T_1 T_2(\omega_0^2 + \omega^2 + T_2^{-2})} \quad (3)$$

$$M_z = \frac{[4\omega^2 + T_2^2(\omega_0^2 - \omega^2 + T_2^{-2})^2] M_0}{4\omega^2 + T_2^2(\omega_0^2 - \omega^2 + T_2^{-2})^2 + \frac{1}{2}\gamma^2 H_1^2 T_1 T_2(\omega_0^2 + \omega^2 + T_2^{-2})} \quad (4)$$

The resonance frequency is

$$\omega_0 = \gamma H_0$$

and at resonance we have

$$\frac{M_z}{M_0} = \frac{\mu''}{\mu''_0} = \left(1 + \frac{1}{4} \gamma^2 H_1^2 T_1 T_2 \right)^{-1} \quad (5)$$

where M_0 is the d-c magnetization and μ''_0 the susceptibility at resonance for vanishingly small microwave amplitude. The value of T_2 is determined by the inverse width of the magnetic resonance line. Then T_1 can be determined from equation (5) by measuring μ'' and M_z as a function of H_1 . It is seen that μ'' and M_z should be proportional. The experimental results are in good agreement with equation (5), as shown in Figure 4. To obtain the observed change $M_z - M_0$ in absolute value, the pick-up coil system had to be calibrated. This was done by means of a test coil, consisting of two windings of known area. A calibrated fast current pulse was passed through it. Uncertainties in the geometry make the method rather inaccurate. Alternatively, we can calculate M_0 from the known susceptibility and weighed amount of paramagnetic salt, and then assume the proportionality between M_z and χ'' . This latter calibration of the pick-up coil is more accurate and was used in the other experiments. It agreed, however, within 30% with the test coil method. The characteristic time with which M_z approaches its steady state value of equation (4) is given by

$$\tau = \left(T_1^{-1} + \frac{1}{4} \gamma^2 H_1^2 T_2 \right)^{-1} \quad (6)$$

It is seen that the decay should be more rapid the larger H_1 . The true relaxation time can only be obtained from the trailing edge of the edge of the magnetron pulse, when $H_1 = 0$. These findings are confirmed by the experimental recordings. At room temperature the experimental decay is not determined by the relaxation time, but by the characteristic time of the apparatus.

The experimental results for the spin-lattice relaxation time by the various methods are tabulated in Table I.

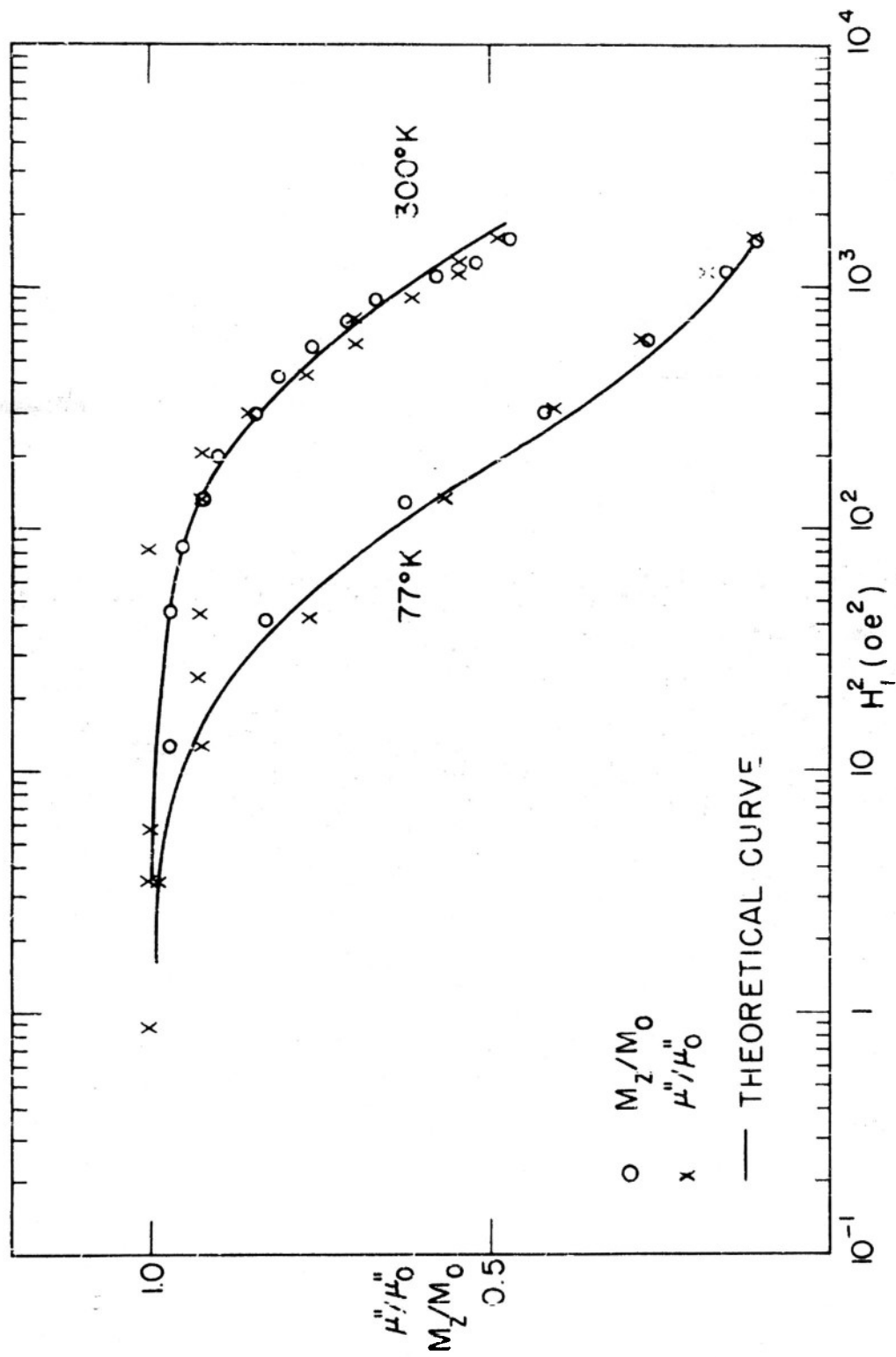


Fig. 4. The imaginary part of the microwave susceptibility χ'' and the z-component of magnetization M_z , as a function of microwave field strength H_1 at resonance², for $MnSO_4 \cdot 4H_2O$ at room temperature and liquid nitrogen temperature. The drawn curve is given by equation (5).

Relaxation Time T_1 in $MnSO_4 \cdot 4H_2O$

<u>Method</u>	<u>T_1 at 300°K</u>	<u>T_1 at 77°K</u>
Non-resonant dispersion*	1.0×10^{-7} sec	1.3×10^{-6} sec
Saturation of χ''	0.78×10^{-7}	1.2×10^{-6}
Saturation of M_z	0.78×10^{-7}	1.2×10^{-6}
Time variation of M_z		1.2×10^{-6}

The substantial agreement between the various methods gives confidence in our experimental procedure.

II.

Paramagnetic Relaxation with Exchange

New results are obtained when these methods are applied to material with a considerable exchange energy.

Although saturation experiments were first carried out for ferromagnetic materials below the Curie point, we shall in this paper first present the results obtained in the paramagnetic region for some ferrites, an organic free radical and an anhydrous ferric salt. The theory for the relaxation above the Curie point is much better understood and the experimental results can be satisfactorily accounted for. In Figure 5a the d-c magnetization M_z and the microwave susceptibility χ'' for the free radical α - α diphenyl- β -picrylhydrazyl are plotted as function of the square of the microwave amplitude. The width of the resonance line is narrowed by exchange interaction, the Curie temperature¹¹ being in the neighborhood of 60°K. The second moment of the line in the polycrystalline material is 1.45 oersted,¹² while Hutchisson¹³ recently found 0.95 oersted for a single crystal. There is apparently some anisotropy broadening in the powder. It is seen that the saturation is 50% complete when the linear microwave

*The ρ used by Gorter¹ e. a. is defined in such manner that $\rho = 2\pi T_1$.

field is 1.8 oersted or approximately a factor two larger than the linewidth. For amplitudes of 10 gauss or more nearly complete saturation occurs. The d-c magnetization and χ'' are almost zero. The magnetization of the free radical then precesses in an equatorial plane perpendicular to the direction of H_0 . The curves for M_z and χ'' coincide and follow the descriptive equation (5) very well. Taking $T_2 = 6.0 \times 10^{-8}$ sec we obtain $T_1 = 6.4 \times 10^{-8}$ sec. Thus T_1 and T_2 are equal, independent of the temperature, and both determined by the exchange narrowing of the dipolar interaction, as will be discussed more fully below. For anhydrous ferric sulfate (Curie temperature $T_c = 70^\circ\text{K}$) an incipient saturation was observed for χ'' at the highest obtainable microwave power level. The value of χ'' dropped to 95% of its value at low fields for $H_1 = 40$ gauss. More conclusive results could not be expected as the exchange narrowed width is 90 gauss, and still higher levels would be needed for saturation. The data for linewidth and saturation in $\text{Fe}_2(\text{SO}_4)_3$ can be described by equation (5), taking $T_1 = T_2 = 6.3 \times 10^{-10}$ sec.

Figure 5b finally shows some data at 200°C for a nickle zinc ferrite (11.4%NiO, 38.6%ZnO, 50% Fe_2O_3) with a Curie temperature of 40°C and manganese zinc ferrite (14.9%MnO, 1.5%FeO, 15.6%ZnO, 67.9% Fe_2O_3) with a Curie temperature of 137°C . Again the results are satisfactorily described by equation (5). The linewidth is 140 oe or $T_2 = 4.1 \times 10^{-10}$ sec, and $T_1 = 9.11 \times 10^{-10}$ sec. There is some uncertainty in the normalization of the M_z curve. Only the difference $M_z - M_0$ is measured. For the organic free radical, complete saturation, for which $M_z = 0$, was attained. So M_0 could be determined in that case. For the ferrites no experimental data on the magnetization above T_c are available, but a calculation with Neel's formula for the susceptibility of a ferrimagnetic substance above the Curie point has been used and gave reasonable agreement between the M_z and μ'' curve.

The basic idea of the theory for the linewidth with exchange narrowing first suggested by Gorter and Van Vleck^{14,15}, is that the dipolar interaction is randomly modulated by the exchange interaction in much the same way as it is modulated by random motion in liquids.² In the latter case the

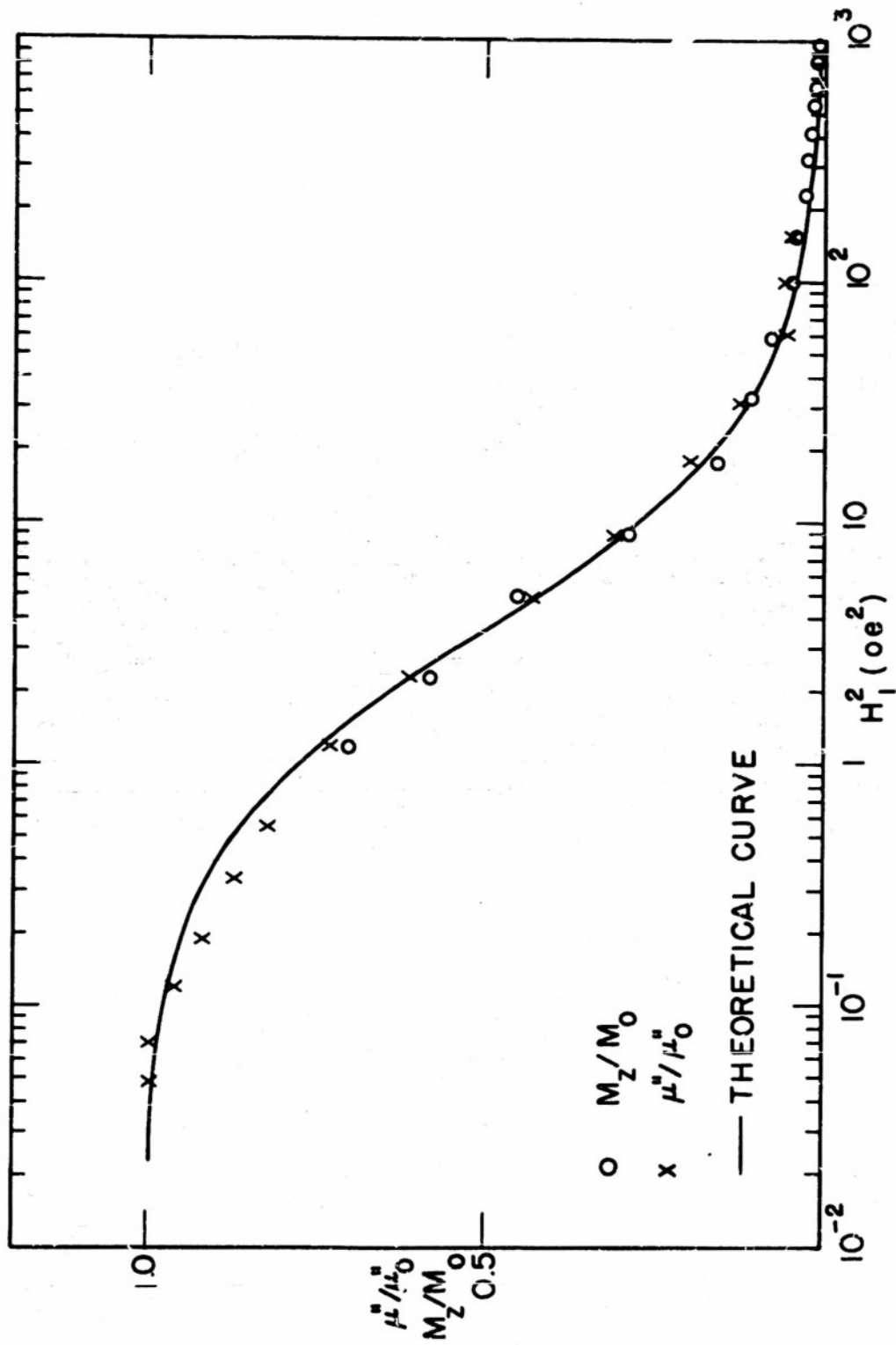


Fig. 5a. The quantities μ'' and M_Z as a function of microwave field strength H_1 for α - a diphenyl β -picryl hydrazyl at 300°K. Substantially the same results were obtained at 77°K. The drawn curve is given by equation (5).

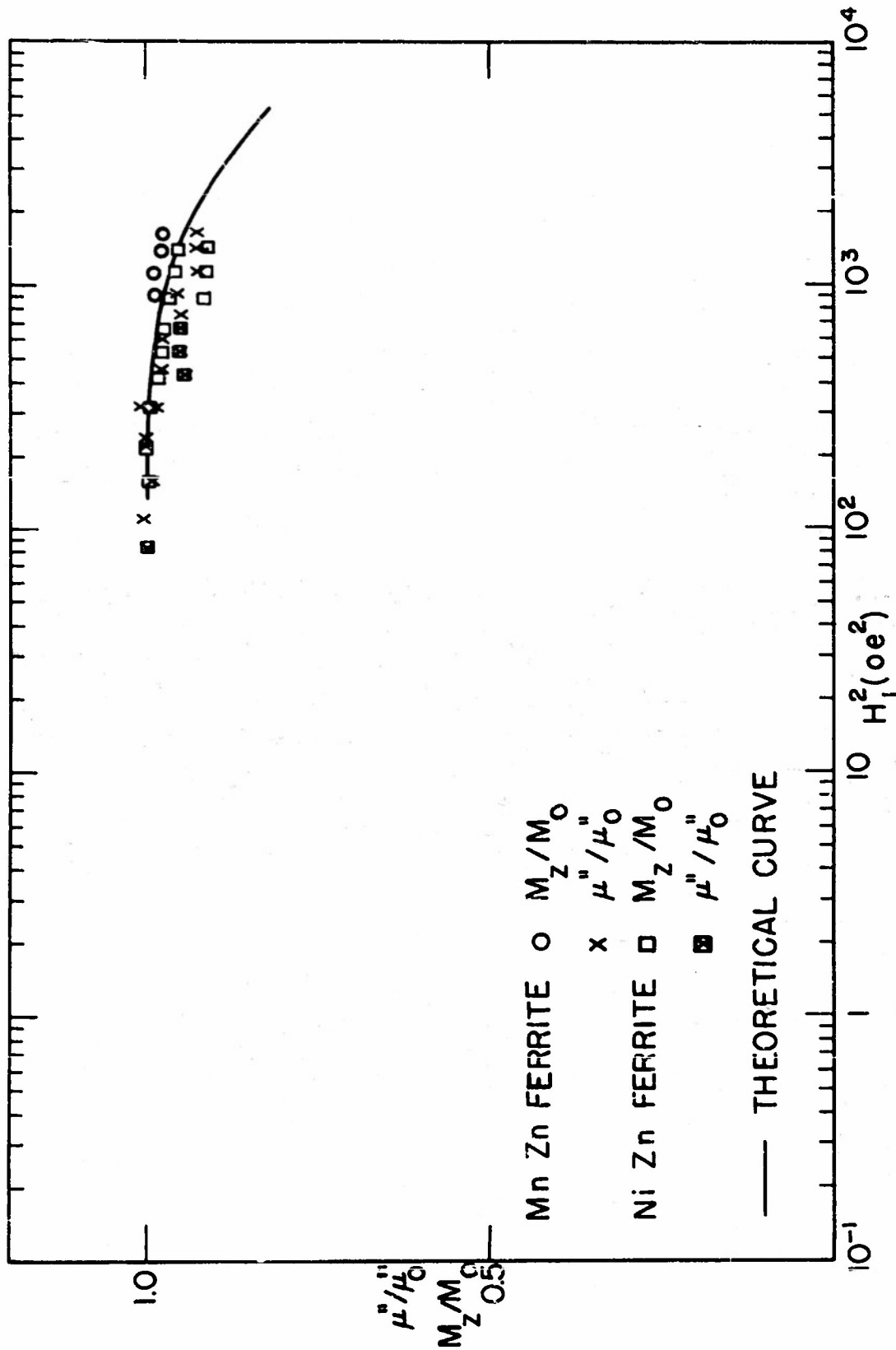


Fig. 5b. The quantities μ'' and M_z for two ferrites at 200°C as a function of microwave field strength H_1 . Nickel zinc ferrite (curve A) has a Curie temperature of 40°C; manganese zinc ferrite (curve B) has a Curie temperature of 137°C.

radius vector connecting a pair of dipoles varies in a random fashion. The exchange interaction modulates the spin orientation rather than the spatial coordinates. The Hamiltonian for this problem, which has been discussed in great detail by Anderson and Weiss,¹⁶ can be written as

$$\mathcal{H} = \mathcal{H}_0 + \mathcal{H}_{\text{exch}} + \mathcal{H}_{\text{dip}} \quad (7)$$

Here \mathcal{H}_0 represents the energy in the external magnetic field

$$\mathcal{H}_0 = g\beta H_0 \sum_j S_{zj} \quad (8)$$

The exchange energy and the energy between classical magnetic dipoles are given by

$$\mathcal{H}_{\text{exch}} = 2 \sum_{i>k} J_{ik} S_i \cdot S_k \quad (9)$$

$$\mathcal{H}_{\text{dip}} = g^2 \beta^2 \sum_{k>j} \left[r_{kj}^{-3} S_j \cdot S_k - 3 r_{jk}^{-5} (r_{jk} \cdot S_j)(r_{jk} \cdot S_k) \right] \quad (10)$$

The case of interest here is when

$$\mathcal{H}_{\text{exch}} \gg \mathcal{H}_0$$

$$\mathcal{H}_{\text{exch}} \gg \mathcal{H}_{\text{dip}}$$

Note that $\mathcal{H}_{\text{exch}}$ commutes with \mathcal{H}_0 , but \mathcal{H}_{dip} does not commute with either \mathcal{H}_0 or $\mathcal{H}_{\text{exch}}$. In a magnetic resonance experiment the magnetic energy \mathcal{H}_0 is increased by the absorption of quanta

$$\hbar\omega_0 = h\nu_0 = g\beta H_0 \quad (11)$$

By a relaxation process this absorbed energy is eventually transferred to the lattice. In this case of large exchange energy it is possible that the dipolar interaction first transforms the magnetic energy into exchange energy rather than directly to the lattice. The situation is entirely analogous to the relaxation in liquids. There the thermal motion randomly modulates the dipolar interaction. A narrow line results and in the relaxation process

magnetic energy is converted into thermal energy of the Brownian motion, with a T_1 about equal to T_2 . Here the exchange energy modulates the dipolar interaction. A narrow line results, and in the relaxation process magnetic energy is converted into exchange energy, with a relaxation time T_1 about equal to T_2 . The terms in the dipolar interaction which connect the states $S_z + 1$, $S_z + 2$ with the state S_z are responsible for the relaxation. Keffer¹⁷ and Anderson¹⁶ have noted, these terms must also be included in the calculation of the width. They must of course be excluded when $\mathcal{H}_{\text{exch}} < \mathcal{H}_0$. Then relaxation by conversion into exchange energy is not possible, and we have the spin-lattice relaxation of normal paramagnetic salts.

The specific heat connected with the exchange energy of the spin system is so much larger than that connected with the magnetic energy, that the exchange spin system can act like a heat reservoir for the magnetic degree of freedom. We can next ask how the energy is eventually dissipated from the exchange spin system to the crystalline lattice. This will presumably occur in a process in which a quantum of the order of the exchange energy J is transferred to one or two lattice phonons. The dipolar interaction will again connect the initial and final states. The relaxation time for this process will however remain unobservable as can be shown by the following analysis of the balance of energy between the "magnetic system," the "spin exchange system" and the lattice. We introduce the specific heats C_H and C_e and temperatures T_H and T_e for the magnetic and exchange systems respectively, C_H is to be taken at constant magnetic field. Well above the Curie temperature we have¹⁸

$$C_H = CH_0^2 T_H^{-2} = -H_0 \frac{dM_z}{dT} \quad (12)$$

$$C_e = CH_{\text{exch}}^2 T_e^{-2} \quad (13)$$

Where C is Curie's constant in Curie's law for paramagnetism, and $H_{\text{exch}} = J/\beta$. Furthermore, we introduce the relaxation times t_{Hl} , t_{He} and t_{el} for the energy transfer between magnetic system and lattice, magnetic and exchange system, exchange system and lattice respectively. The power absorbed by magnetic system from the microwave field during magnetic resonance is

$$P = \mu'' H_1^2 \omega V / 8\pi = W M_z H_0 \quad (14)$$

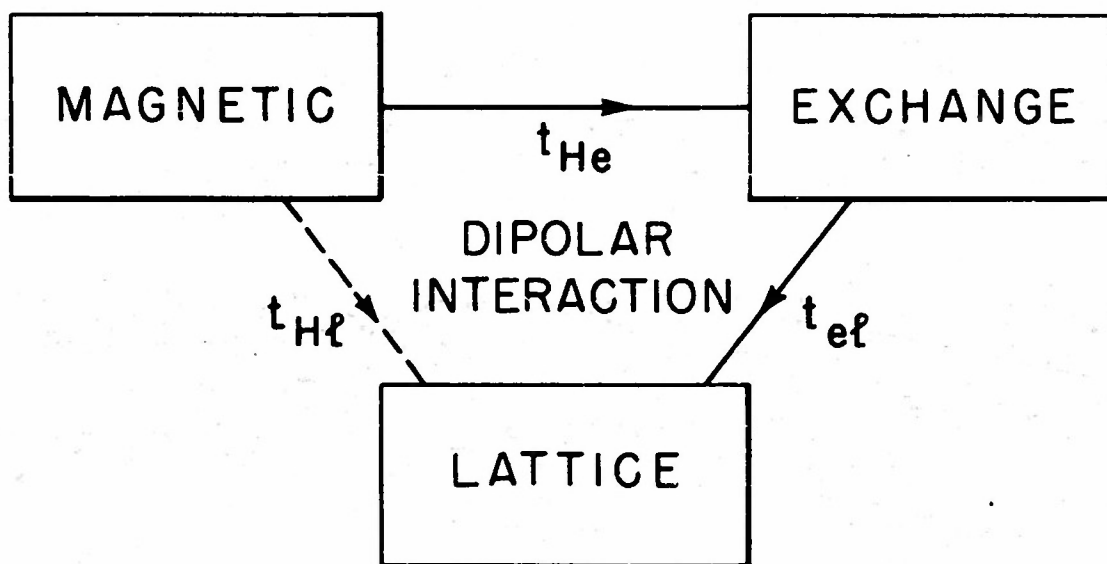


Fig. 6. In a magnetic resonance experiment power is absorbed by the magnetic system. If $H_{ex} \gg H_0$, heat contact with the exchange spin system and the lattice is established by dipolar interaction. The direct contact between the magnetic system and the lattice is usually negligible.

Here W is the transition probability of one spin, proportional to H_1^2 , ω is the angular frequency of the microwave field H_1 , M_z is the magnetization of the sample with volume V . The energy balance for the magnetic system is then expressed by the equation

$$WM_z H_0 = + \frac{C_H(T_H - T_e)}{t_{He}} + \frac{C_H(T_H - T_l)}{t_{Hl}} + C_H \frac{dT_H}{dt} \quad (15)$$

The energy balance for the spin exchange system is

$$0 = - \frac{C_H(T_H - T_e)}{t_{He}} + \frac{C_e(T_e - T_l)}{t_{el}} + C_e \frac{dT_e}{dt} \quad (16)$$

The direct heat contact with the lattice is negligible when $t_{Hl} \gg t_{He}$. Experimentally this appears to be the case, since the saturation effect does not depend on the lattice temperature T_l and is therefore wholly determined by the temperature independent term with t_{He} . A steady state is reached after a time t_{He} or t_{el} , whichever is longer. Then one obtains from equation (15) and (16)

$$P = + \frac{C_H(T_H - T_e)}{t_{He}} = + \frac{C_e(T_e - T_l)}{t_{el}} \quad (17)$$

Since $\frac{C_H}{C_e} \approx \frac{H_0^2}{H_{exch}^2} \approx 10^{-6}$, we find that usually T_e will practically be equal

to T_l , unless t_{el} were a million times longer than t_{He} . The observed change in magnetization is an indication for t_{He} . There is no equilibrium between the magnetic and exchange energy of the spin system during the saturation experiment. The observed characteristic time is t_{He} , with which the phenomenological T_1 must be identified. If the exchange lattice contact were the bottleneck in the energy transfer process, a much slower decay time should have been observed. Actually, it was found that a steady state was established during a one microsecond pulse of the magnetron. The time to reach a steady state is only a fraction of this time. The time t_{el} remains therefore unobservable. The transfer to the lattice takes place in large quanta J , and even if the elementary process for this transfer is not very fast, it can still easily keep up with a rate, at which energy in the form of

small quanta $g \beta H_0$ is pumped into the system. The point of view given here is similar to that developed independently by Anderson for this paramagnetic case. The experimental results can then be interpreted as an interesting confirmation of the exchange modulation of the dipolar interaction developed by Anderson* and Weiss.¹⁶ The relaxation time in both ferromagnetic and antiferromagnetic materials above the Curie temperature is equal to the inverse line width.

The non-resonant experiments of the Dutch school¹ usually gave negative results for paramagnetic salts with a large exchange energy which is ascribed to the high specific heat of the spin system which included both magnetic and exchange energy in those considerations. In the thermodynamical theory of Casimir and DuPre these were assumed to be in equilibrium.¹⁹ It is clear from the foregoing discussion that if the exchange energy is sufficiently large and the line sufficiently narrow, a relaxation effect may be observed around a frequency equal to the inverse line width. At higher frequencies the magnetization will not be in equilibrium with the exchange energy. In a - a diphenyl- β picryl-hydrazyl this would occur in the convenient frequency range around 10 Mcs.

Although the relaxation process discussed here occurs entirely within the spin system and should therefore be called a spin-spin relaxation, it has the special characteristic of spin lattice relaxation, that magnetic energy is not conserved.

III

Ferromagnetic Relaxation Effects

We now turn to the experimental results when ferrites and supermalloy below their Curie temperatures are subjected to high microwave amplitudes.

Nickel ferrite - Single crystals of $\text{NiO} \cdot \text{Fe}_2\text{O}_3$ were kindly supplied by the Bell Telephone Laboratories. The samples were ground to a spherical shape with a diameter of less than 1 mm. They could be mounted at the

* The authors are indebted to Dr. Anderson for sending his unpublished notes.

cavity wall or on a polyfoam stick. It was shown by variation of diameter and position, that the effects of size and proximity of the cavity walls were negligible.

The value of μ''/μ_0'' at resonance is plotted in Figure 7 as a function of the microwave power for a range of temperature between 77°K and 725°K. In the same figure we have also plotted M_z/M_0 at two temperatures for comparison. The most striking characteristic is that the M_z and μ'' do not coincide, as required by equation (5), below the Curie point. The curves approach each other more and more as the temperature is raised, and they do coincide in the paramagnetic region. The Curie temperature of nickel ferrite is 600°C, and we could not take data above this temperature, but such data have been obtained for ferrites with a lower Curie point. We wish to emphasize the fact that in previous publications the change in M_z was reported 10 times too large due to a regrettable error in the calibration. In fact the total relative variation in the magnetization is never larger than 6% in ferromagnetic materials. Since these small changes do not show up very well in Figure 7, we have replotted the variation ($M_0 - M_z$) as a function of the actually absorbed power P in Figure 8. The quantity P is directly observed experimentally. From it μ'' is derived with the aid of equation (14). It is seen that a linear relationship exists between P and $M_0 - M_z$ at all temperatures. The direct observation of the changes in M_z always yielded pictures like the one reproduced in Figure 2. From this it can be inferred that a steady state is reached during each pulse and that the relaxation time for the magnetization to return to equilibrium is shorter than 2×10^{-7} sec.

The question now arises how to interpret the μ'' and M_z saturated curves. A clue to the decrease in μ''_{\max} without a concomitant decrease in M_z is given by the behavior off resonance. An extra absorption begins to occur in the tails as H_1 increased, especially on the low field (high-frequency) side of the resonance. At very high field strengths even a secondary maximum is developed. These broadening effects exhibited in Figure 9 are more pronounced at lower temperatures. They disappear gradually and completely near and above the Curie point.

The change in M_z seems to be proportional to the absorbed power under all circumstances. It shows the same secondary maximum as a function of

H_0 as μ'' . Whatever the cause of the unexpected variation of the ferromagnetic resonance curve with incident power may be, a general argument about the conservation of energy can be given, as was first pointed out by Anderson²⁰ and developed in the preceding section. The actually absorbed power can again be dissipated from the magnetic system via the exchange spin system, or directly to the lattice. In terms of the spin wave language of ferromagnetism, we can say that very long spin waves with wave number near zero are created by the external microwave field. As $M_x H_1$ commutes with the exchange energy, the latter cannot change during the microwave absorption process. These long spin waves which have only magnetic energy then collide with other spin waves, whose exchange energy is increased. The collision process consists of a transformation of magnetic energy into exchange energy by dipolar or pseudo-dipolar interaction. The shorter spin waves are eventually destroyed in collisions with the lattice phonons. Direct collisions of the long spin waves with the lattice are unlikely so we can neglect the term with $t^{-1} H_0$ in equation (15). A further discussion of the spin wave theory of relaxation will be given in section IV.

The thermodynamic equations (15), (16) and (17) are still valid, provided we take for the specific heats the values which obtain well below the the Curie temperature

$$C_H = - H_0 \frac{\partial M}{\partial T} \quad (18)$$

$$C_e = - \alpha M \frac{\partial M}{\partial T} = - H_{\text{exch}} \frac{\partial M}{\partial T} \quad (19)$$

where αM is the effective Weissfield.

The ratio of the specific heats is now

$$\frac{C_e}{C_H} = \frac{H_{\text{exch}}}{H_0} \sim 10^{+3}$$

The expressions for the specific heat and the magnetization as a function of temperature in the phenomenological Weiss theory and the spin wave theory can be found in many texts on ferromagnetism.^{21,22} Again the bottleneck of energy transfer appears to be between the magnetic and the exchange system. The relaxation time, obtainable from equation (17), to

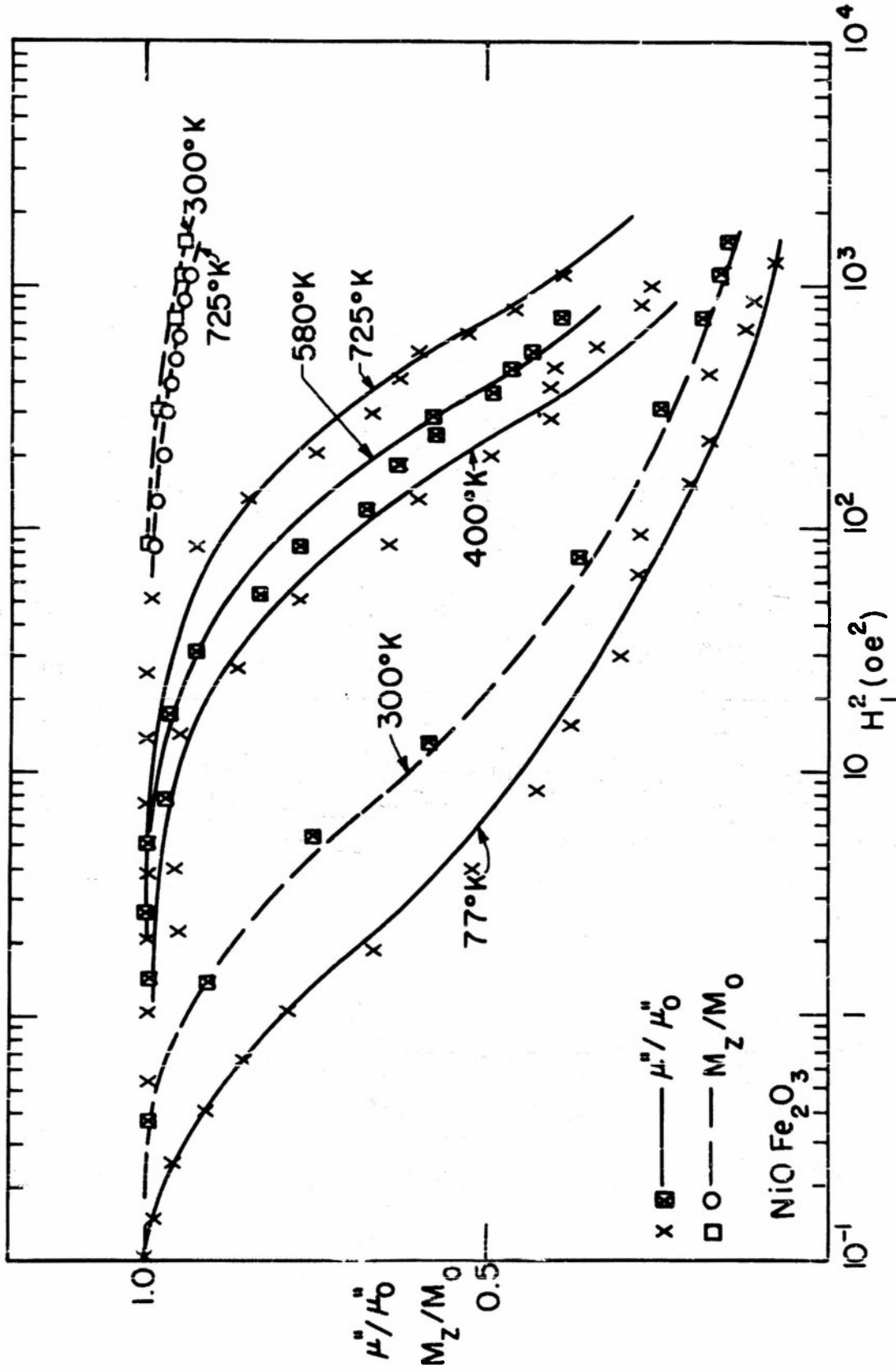


Fig. 7. The value of μ''/μ_0'' and M_z/M_0 (dashed curve) at resonance in a single crystal of nickel ferrite, as a function of H_1^2 for various temperatures.

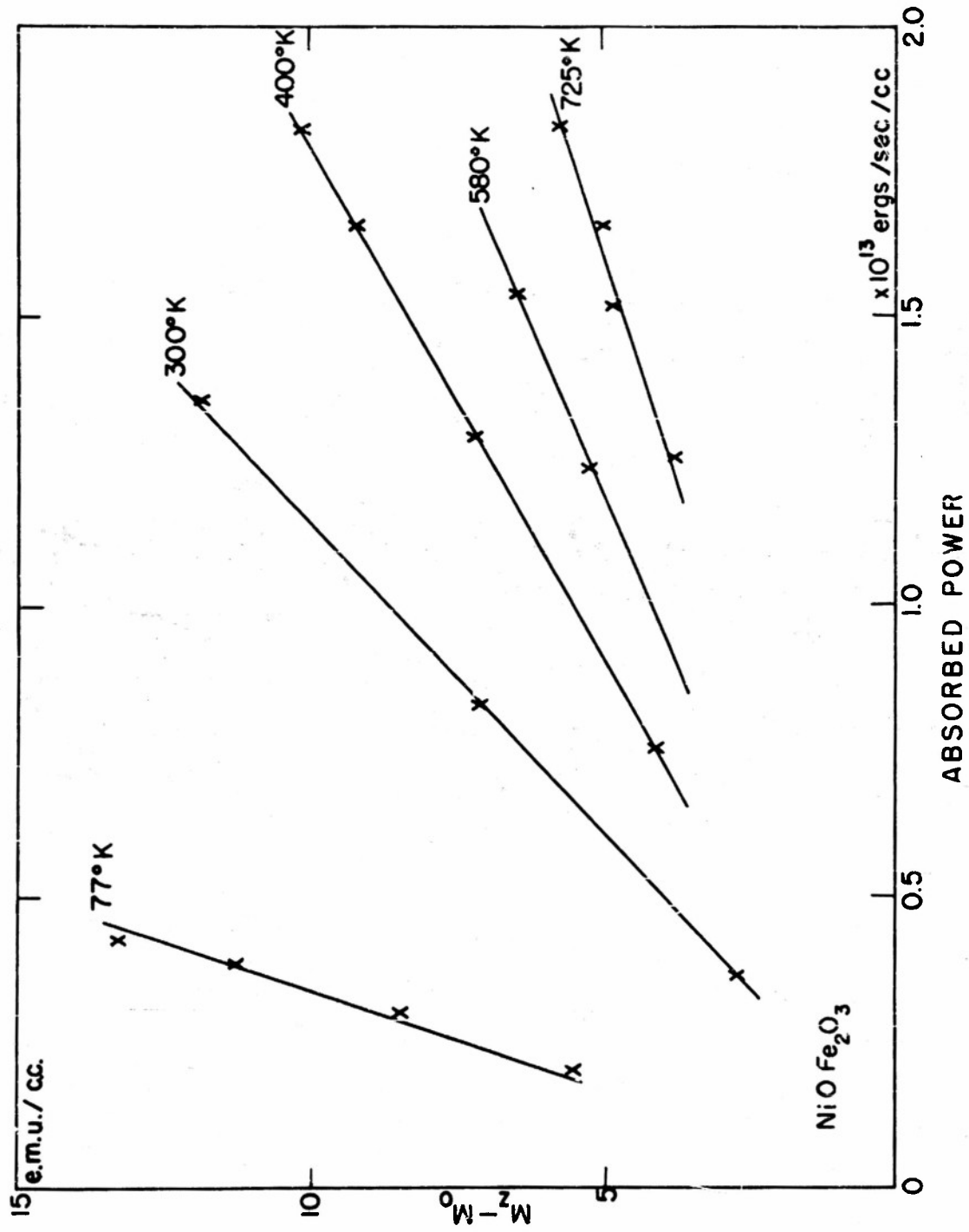


Fig. 8. The change produced in the z-component of the magnetization as a function of the absorbed microwave power in a single crystal of nickel ferrite.

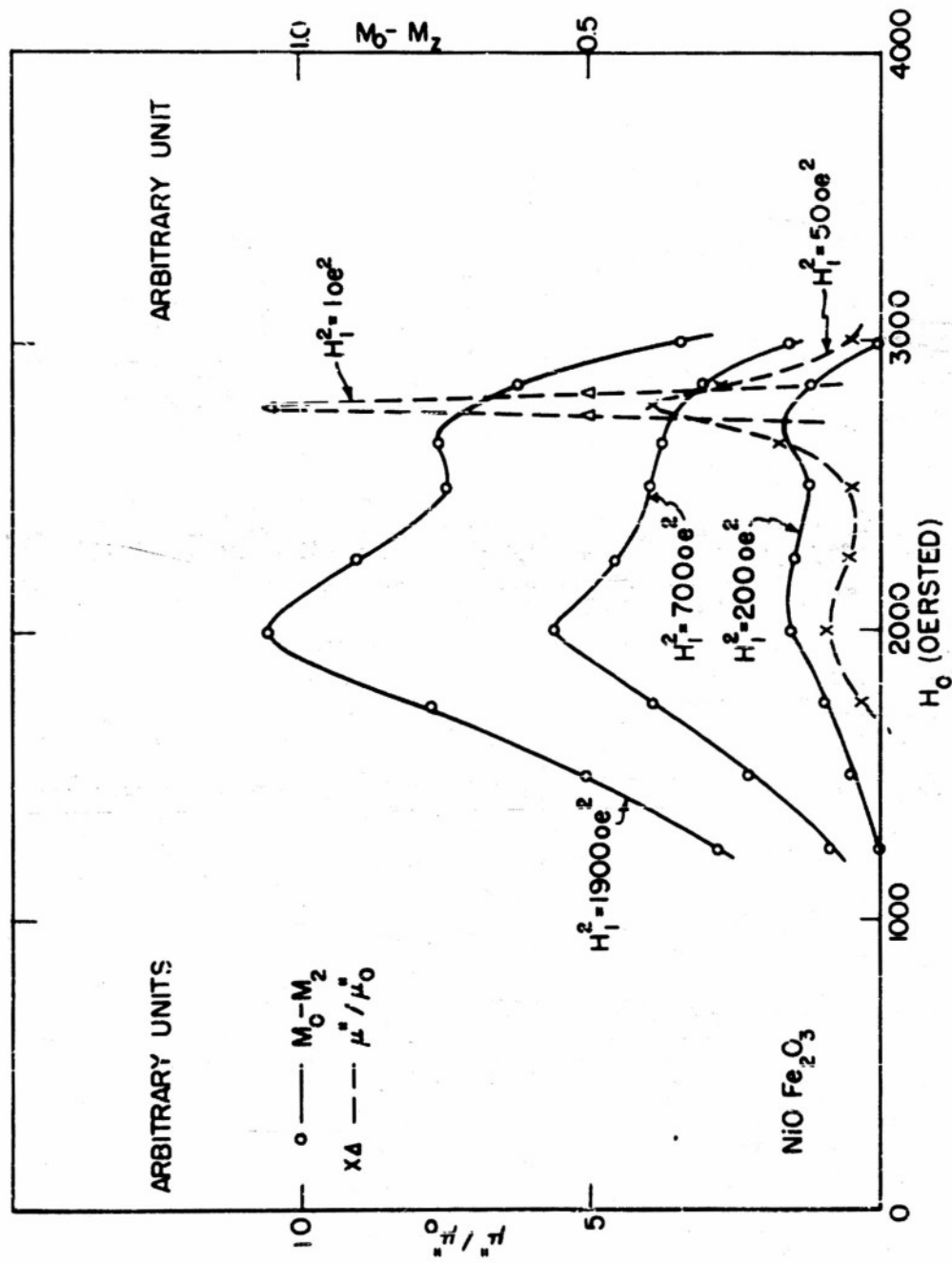


Fig. 9a. The value of μ'' and $M_0 - M_2$ as a function of the d-c magnetic field H_0 . At high microwave power levels an anomalous absorption appears, especially at the low field side of the resonance. These anomalous effects have been observed for a range of temperatures and microwave amplitudes. They disappear gradually near the Curie temperature. At 300°K .

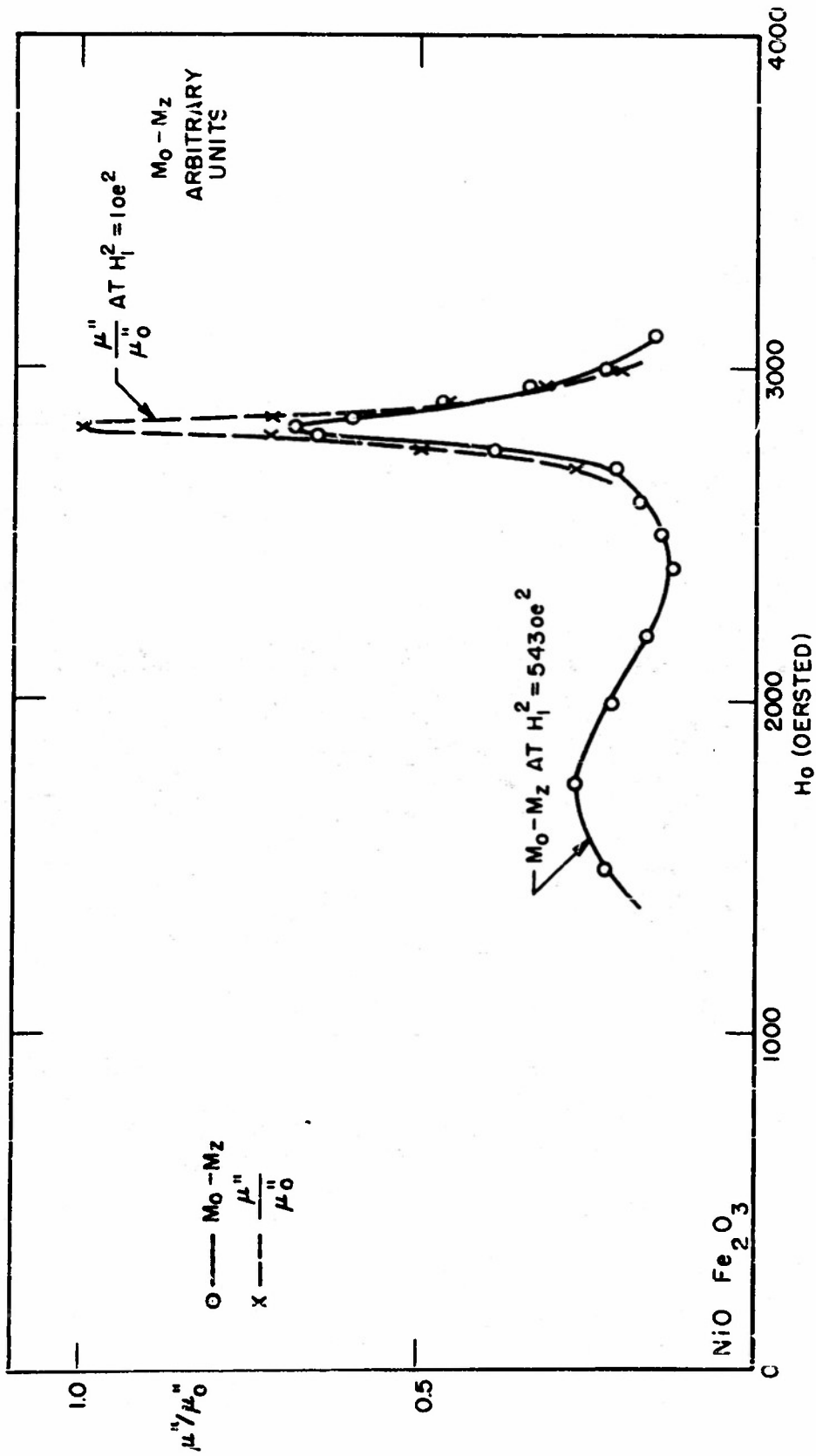


Fig. 9b. The value of μ'' and M_z as a function of the d-c magnetic field H_0 . At high microwave power levels an anomalous absorption appears, especially at the low field side of the resonance. These anomalous effects have been observed for a range of temperatures and microwave amplitudes. They disappear gradually near the Curie temperature. At 580°K .

reach equilibrium between these systems is given by

$$t_{He} = H_0 (M_e - M_H) / P = H_0 (M_0 - M_z) / P \quad (20)$$

The slope of the lines in Figure 8 is a measure for the relaxation time, which is plotted as a function of temperature in Figure 10. It is constant near the Curie temperature, and about equal to the characteristic time derived from the line width ($\Delta H = 37$ gauss). At low temperatures the relaxation time is approximately inversely proportional to T , but the line does not become narrower!

If we assume instead that the line width still is a measure for t_{He} and that the bottleneck for energy transfer is between the exchange system and the lattice, we would find

$$t_{el} = H_{exch} (M_0 - M_z) / P > 10^{-6} \text{ sec.}$$

This is clearly incorrect, as direct observation of the magnetization decay shows that the relaxation time is shorter than 2×10^{-7} sec. The total power absorbed during one microsecond pulse would not be sufficient to heat the whole spin system to such a temperature, as would correspond to the observed change of several percent in M_z . Although the absorbed power is sufficient to raise the temperature of spin system - and also of the whole ferrite lattice which has a comparable specific heat at 77°K , at a rate of about $10^{7^\circ}\text{C}/\text{sec}$, the rise during one pulse would be only a few degrees with a negligible change in M_z . We therefore conclude that the relaxation effect must occur within the spin system and that the thermal equilibrium between the various spin waves is upset during the saturation experiments. Damon⁵ has shown that the μ'' and M_z vs. H_0 curves are displaced but retain their shape when the single crystal is rotated. The crystalline anisotropy field is only a few hundred gauss. Results on powdered samples are essentially the same as those for single crystals.

In addition to nickel ferrite we have investigated three other ferrites, obtained through the courtesy of Philips Research Laboratories, Eindhoven, Netherlands, which are described as follows.

For nickel zinc ferrite, sample 1 (35% NiO, 15% ZnO, 50% Fe_2O_3 ,

Curie temperature 415°C) gave results essentially similar to nickel ferrite. In sample 2 (11.4% Ni, 38.6% ZnO, 50% Fe_2O_3 , Curie temperature 90°C), while no saturation effects could be obtained at 77°K , a large relaxation effect was found at 300°K . The values of μ''/μ_0'' and M_z/M_0 are plotted in Figure 11 as a function of H_1 . The relaxation time t_{He} calculated from equation (20) is given in Figure 10.

Manganese zinc ferrite (14.9% MnO, 15.6% ZnO, 1.5% FeO, 67.9% Fe_2O_3 , Ferrox cube III, Curie temperature 137°C) showed the same behavior as the nickel ferrite. At high microwave power levels μ'' and M_z show double peaks as a function of H_0 . The anomalous absorption at fields lower than the resonance field and the corresponding decrease of μ''_{max} occur again. All these anomalies disappear gradually, if the temperature is increased. The relaxation time calculated from equation (20) with the aid of the results of Figure 14 has the same characteristics as nickel ferrite.

When a plane specimen is used at high power levels a new phenomenon occurs. Since the magnetization changes and since the resonance condition in ferromagnetic media contains the magnetization through the demagnetizing fields, the position of the resonance for a plane slab will depend on the microwave amplitude. Furthermore, the value of H_1 required for a certain degree of saturation depends on the geometry. For a ferromagnetic medium we have to substitute for H into the equations of motion (2) the effective field, containing the demagnetizing and anisotropy fields.²³ Instead of equation (5) we find in first approximation for a ferromagnetic medium²⁴

$$\frac{\mu''}{\mu_0''} = \frac{M_z}{M_0} = \left[1 + \frac{1}{4} \gamma^2 H_1^2 T_1 T_2 \left(1 + \frac{1/2(N_y - N_x)M_z}{H_0 + (N_x - N_z)M_z} \right) \right]^{-1} \quad (21)$$

with

$$\mu_0'' = 2\pi \gamma^2 T_2 \omega_0^{-1} \left[H_0 + (N_y - N_z)M_z \right] \quad (22)$$

and a resonance frequency

$$\omega_0 = \gamma \left[H_0 + (N_x - N_z)M_z \right]^{1/2} \left[H_0 + (N_y - N_z)M_z \right]^{1/2} \quad (22)$$

For a given field H_1 , the amount of saturation M_z/M_0 depends upon the

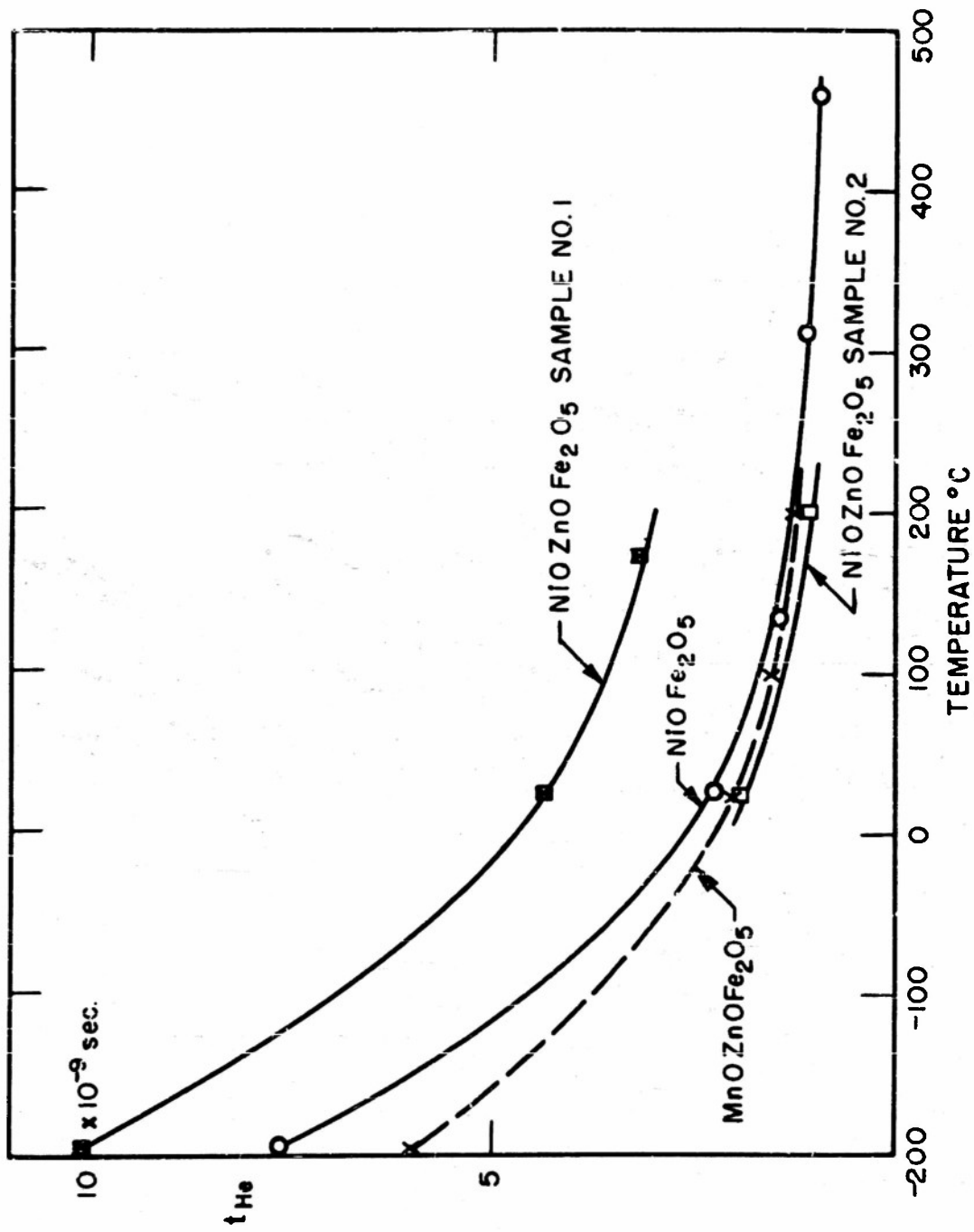


Fig. 10. The relaxation time for the transformation of magnetic into exchange energy, deduced from Figure 8, for nickel ferrite. The same data for manganese zinc ferrite are deduced from Figure 14.

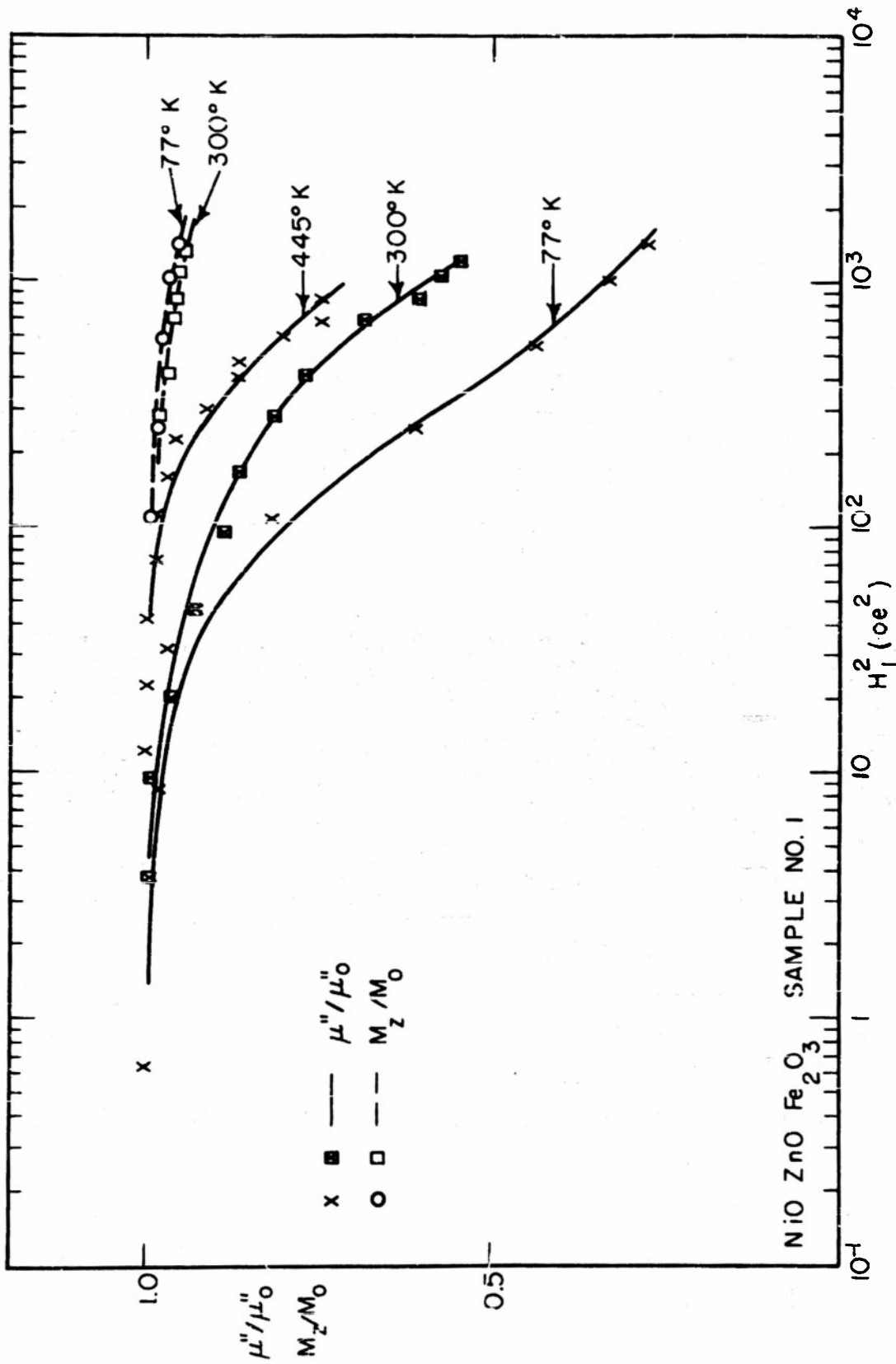


Fig. 11a. The value of μ''/μ_0 and M_z/M_0 (dashed curve) at resonance in polycrystalline nickel zinc ferrite Sample 1 (35% NiO, 15% ZnO, 50% Fe₂O₃)

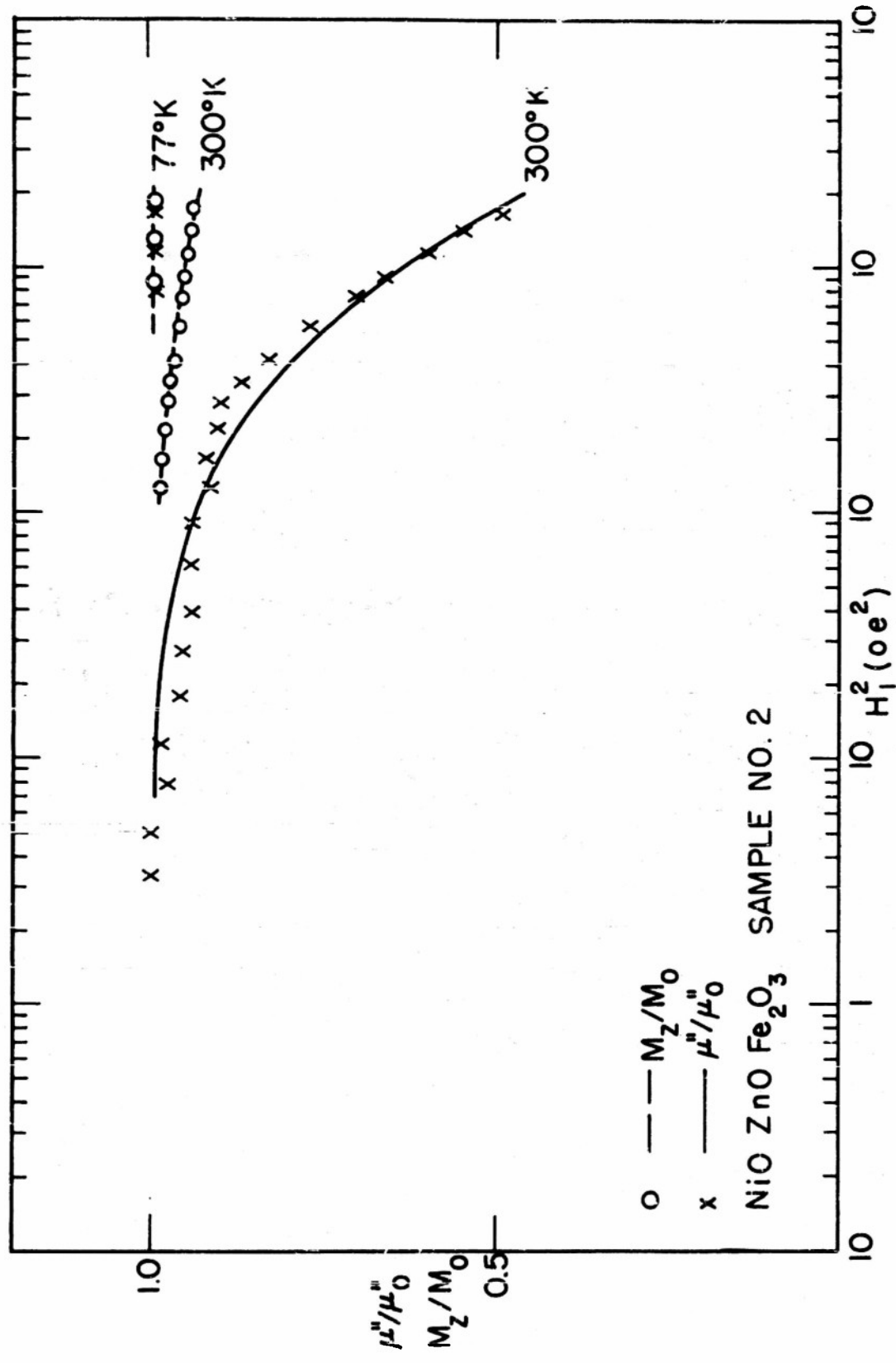


Fig. 11b. The value of μ''/μ_0 and M_z/M_0 (dashed curve) at resonance in polycrystalline nickel zinc ferrite Sample 2 (11.4% NiO, 38.6% ZnO, 50% Fe₂O₃.)

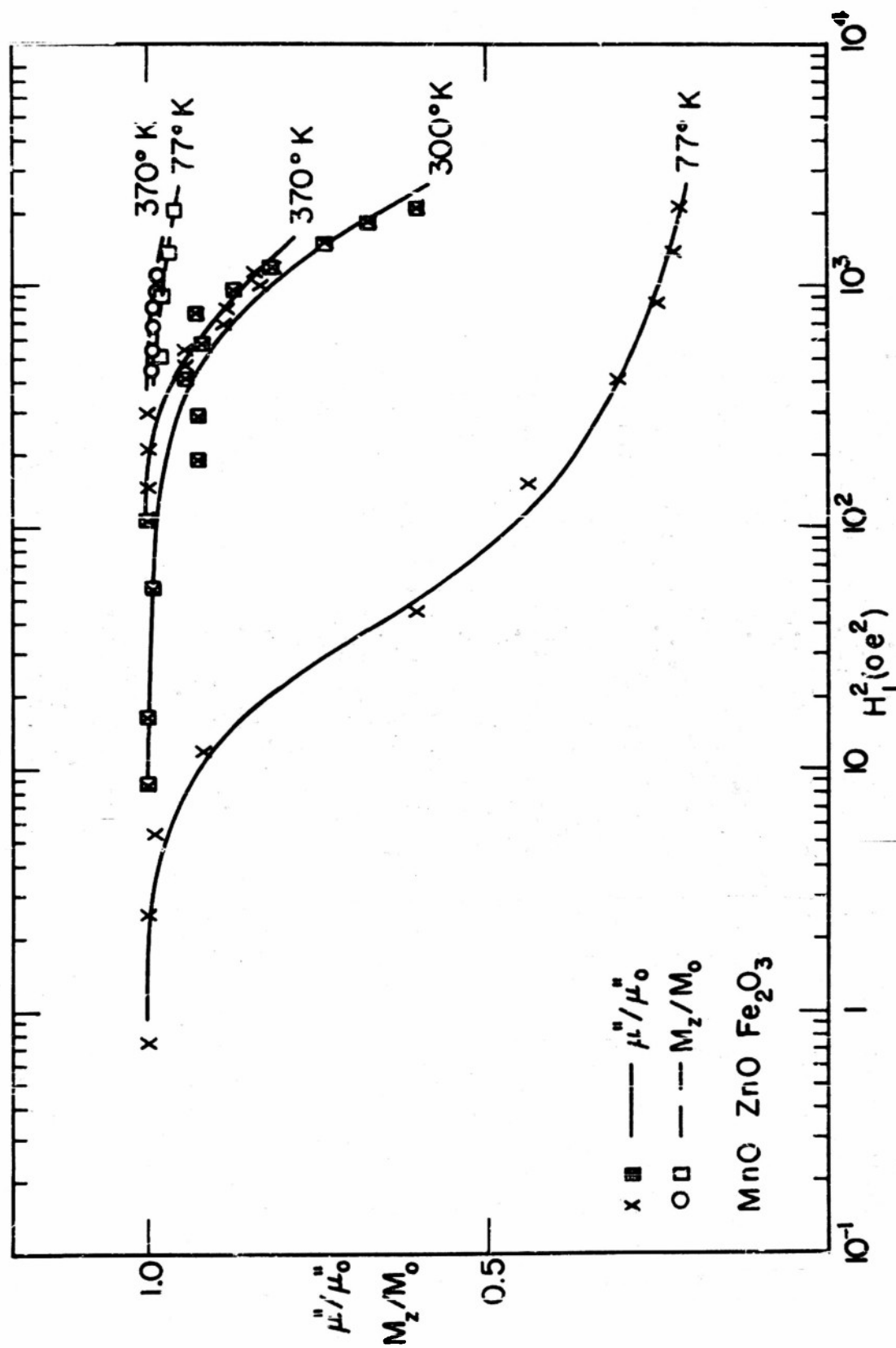


Fig. 12. The value of " μ''/μ_0'' " at resonance in polycrystalline manganese zinc ferrite (14.9% MnO, 15.6% ZnO, 1.5% FeO, 67.9% Fe₂O₃)

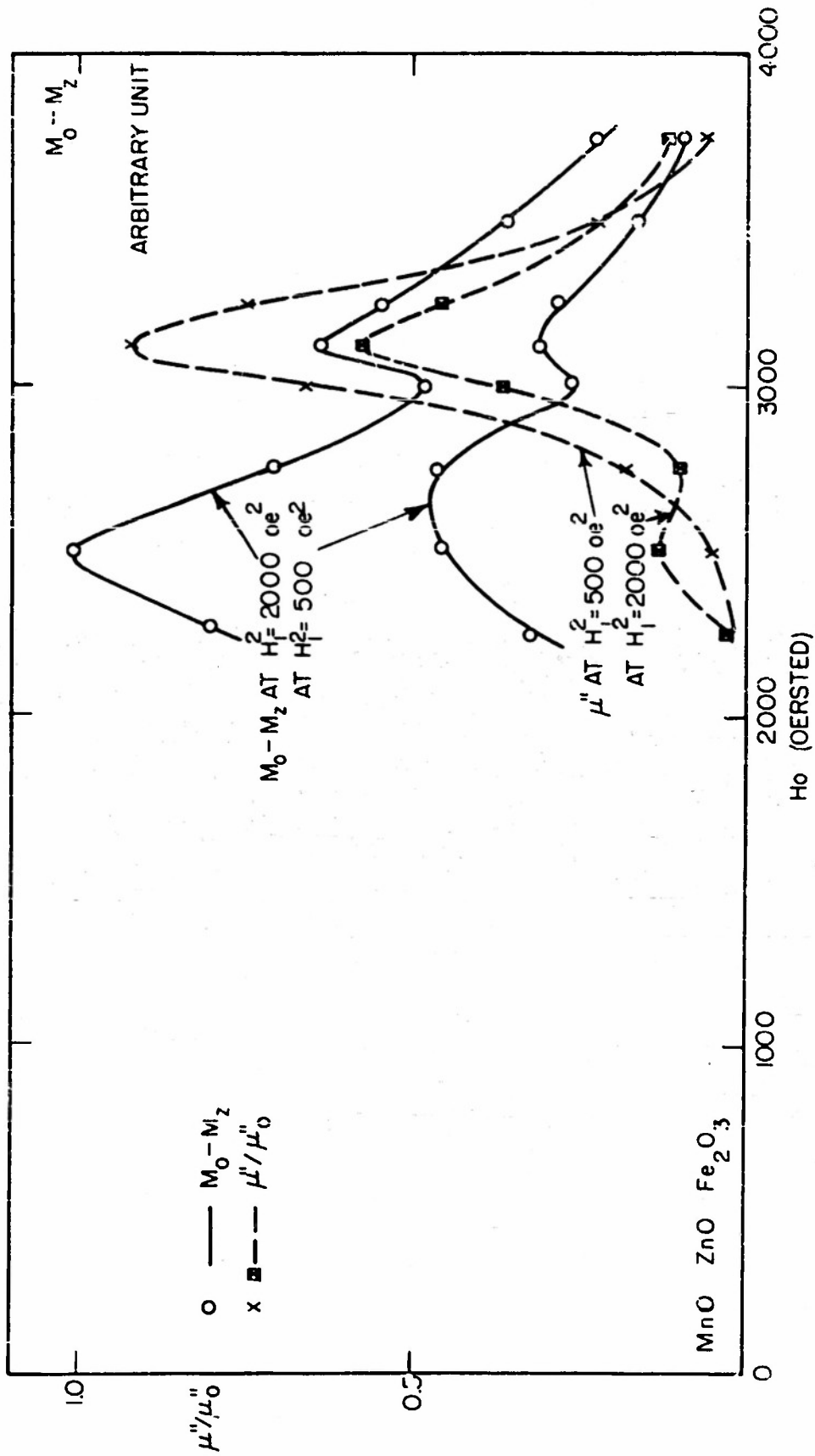


Fig. 13. The value of μ'' and M_z as a function of d. c. magnetic field in polycrystalline manganese zinc ferrite at 25°C.

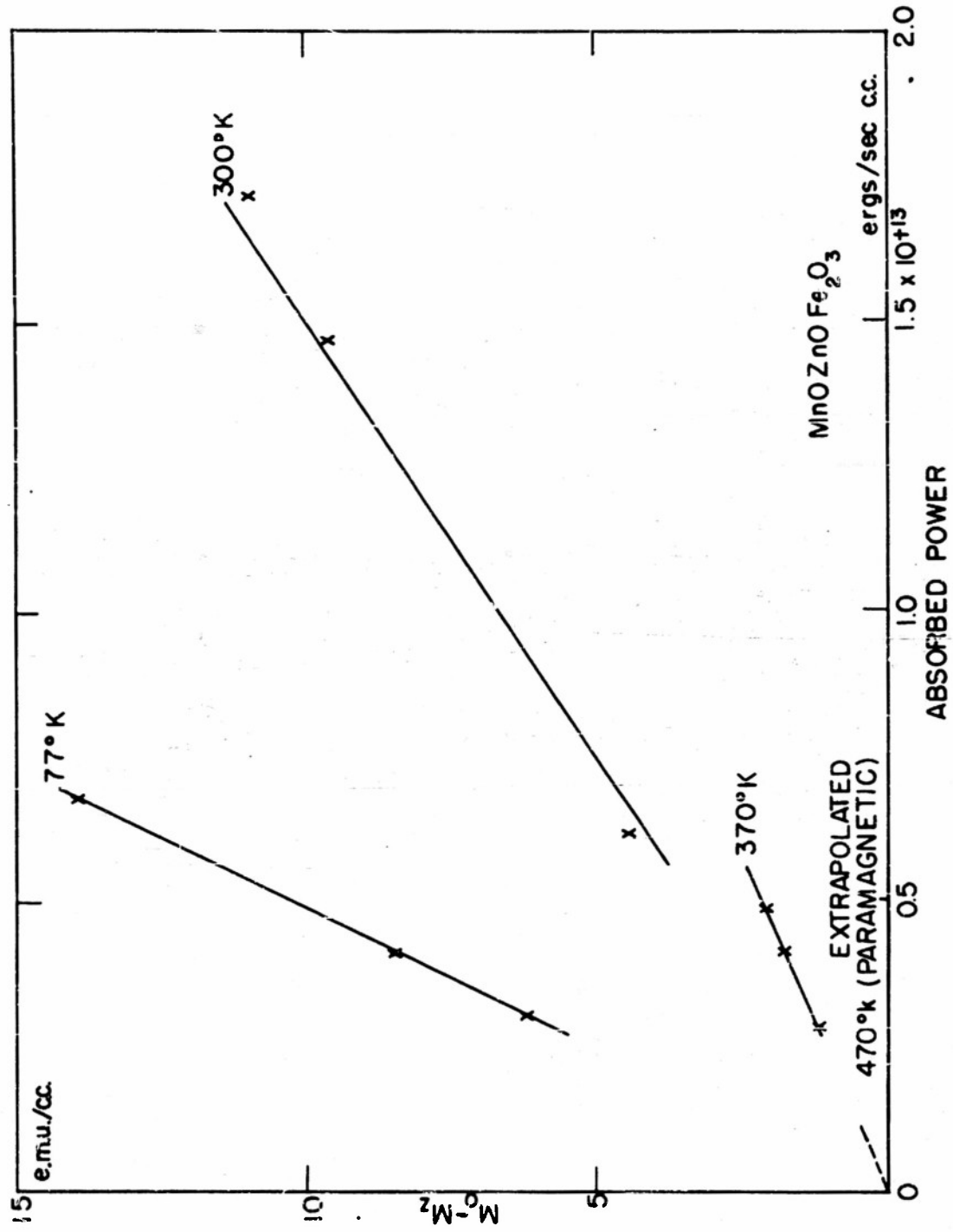


Fig. 14. The value of $M_0 - M_2$ in polycrystalline manganese zinc ferrite as a function of the absorbed power. The slope is a measure of the relaxation time.

geometry. A disk is more easily saturated when H_0 is parallel to the plane ($N_y = 4\pi, N_x = N_z = 0$), than when H_0 is perpendicular ($N_z = 4\pi, N_x = N_y = 0$). For this latter case and for a sphere equation (21) reduces to equation (5) which was derived for paramagnetic materials. Experimentally these shape dependent effects have been observed, as shown in Figure 15.

The shifts of the resonance with microwave power level are in agreement with equation (23) where M_z is calculated from equation (21).

Supermalloy (Curie temperature 400°C), a ferromagnetic metal, has also been investigated for relaxation effects. Because of skin depth effects the geometry is always a flat disk. It can be shown that the skin depth at least at room temperature will not change the relaxation mechanism. At low temperatures with smaller skin depths spin diffusion might become a dominant process. The M_z magnetization could not be picked up directly as the induction is screened by the thickness of the metallic sample. It was impracticable to make the samples so thin that frequencies up to 10^8 cps would pass. However, $M_0 - M_z$ could be determined from the shift of the resonance with power level, although this method is rather inaccurate. The permeability can of course be determined in the usual fashion. The behavior of supermalloy is qualitatively the same as for the ferrites. It is probably characteristic for all ferromagnetic materials and not a special feature of ferrimagnetism in ferrites. For supermalloy the μ'' and M_z curves do not coincide at low temperatures, as shown in Figure 16. The resonance curve in Figure 17 even shows a secondary maximum in the absorption. From the change in M_z , derived from the shift in resonance, and the absorbed power the relaxation time can again be calculated. We find $t_{He} = 1.1 \times 10^{-9}$ sec at 20°C , 0.95×10^{-9} sec at 228°C and 0.74×10^{-9} sec at 335°C . At higher temperatures no saturation could be obtained indicating a very short relaxation time. The dependence of t_{He} on temperature is in fair agreement with the behavior of the line width. 10^6 At all temperatures t_{He} agrees within a factor two with the value of T_2 derived from the width. The decrease of t_{He} and T_2 at higher temperatures is absent in the case of the ferrites. This suggests that the conduction electron play a role in the relaxation mechanism at high temperatures.

In metallic nickel no saturation effects were observable even at the highest power levels. This indicates a relaxation time t_{He} shorter than 5×10^{-10} sec. The value of T_2 derived from the line width is 3×10^{-10} sec at room temperature.

IV

Theoretical Discussion and Conclusions

The damping terms in equation (2) have been introduced in a phenomenological way. Instead of them, another form is frequently used $\lambda \underline{M} \chi [\underline{M} \times \underline{H}] / M_0^2$, which was first introduced by Landau and Lifshitz.²⁵ This particular form of the damping leaves M^2 a constant of the motion and is therefore well suited to describe domain wall motions. As the dipolar interaction does not commute with M^2 , this property is not necessary for damping in ferromagnetic resonance. Both forms give a reasonable description at low microwave fields, provided T_2 , T_1 and λ are given values which change with H_0 . There is evidence from our experiments that M^2 which can be estimated from the observed values of transverse and d-c magnetization, is not conserved for high values of H_1 in ferromagnets well below the Curie point.

It is amusing to calculate what the natural radiation width would be if the rotating magnetization were allowed to radiate in free space. The classical radiation damping of such a macroscopic moment - a "superradiant" state according to Dicke²⁶ as the individual moments are in phase - is surprisingly large. The line width would then be proportional to the volume of the sample and should even be larger than the observed widths. This argument can be dismissed on the grounds that the sample is inside a cavity with which it forms a coupled system. It will not radiate faster than the quality factor of the cavity will permit.

The physical basis for the damping mechanism in ferromagnets was first described by Akhieser²⁷ in terms of collision processes between spin waves^{21,22} and spin-lattice phonons. Let n_k be the occupation number of a spin wave oscillator with wave vector k and energy

$$\epsilon_k = g\beta H_0 + \frac{1}{2} J a^2 k^2 \quad (24)$$

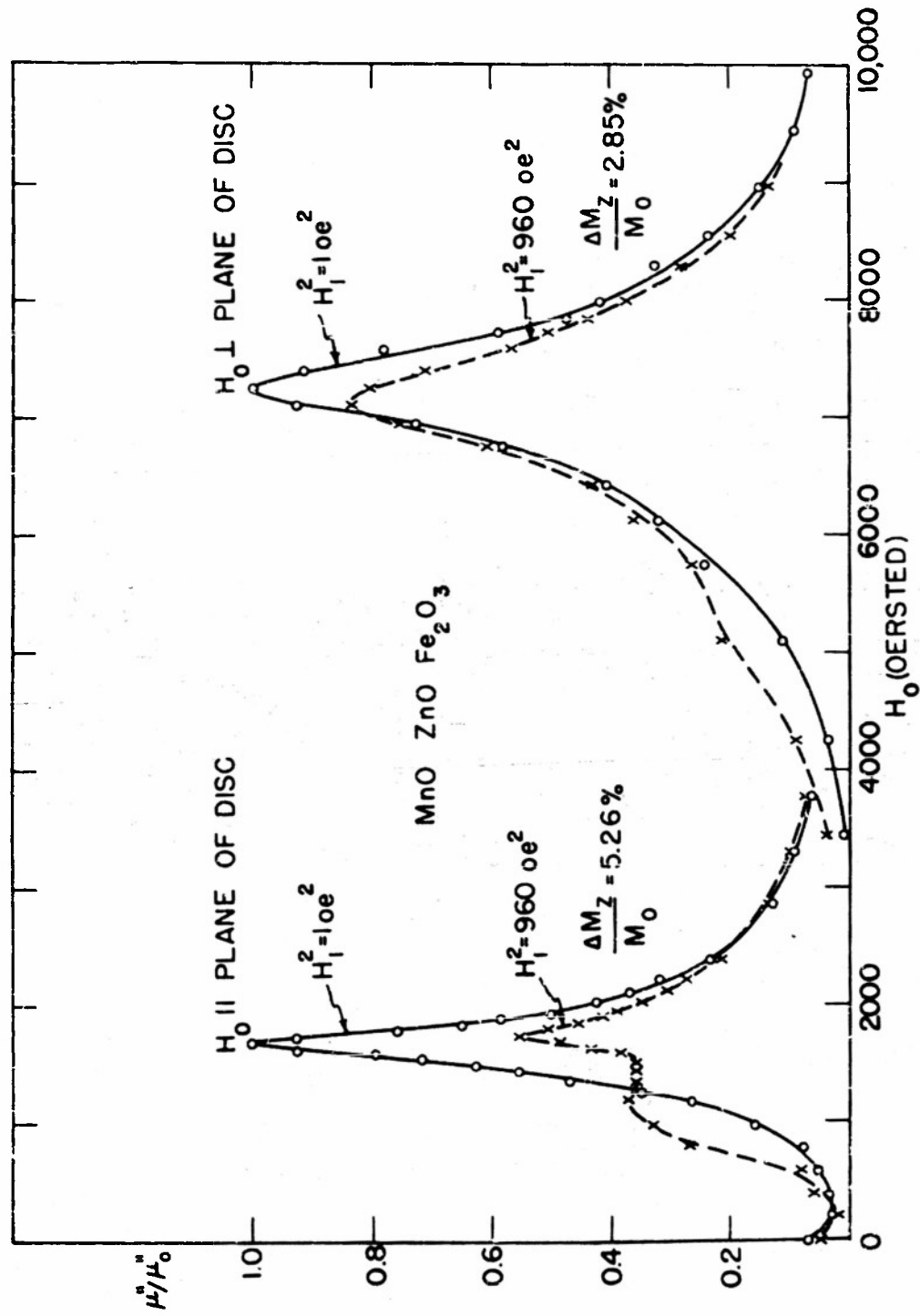


Fig. 15. The Susceptibility μ''/μ_0 in disk-shaped specimen of manganese zinc ferrite. The value of $(M_0 - M_z)/M_0$ at $H_1 = 31$ oersted is also indicated. A different amount of saturation occurs in the two geometries. The resonance at $H_1 = 31$ oersted is displayed toward higher field strength H_0 , when H_0 is parallel to the plane of the specimen and in the opposite direction when H_0 is perpendicular.

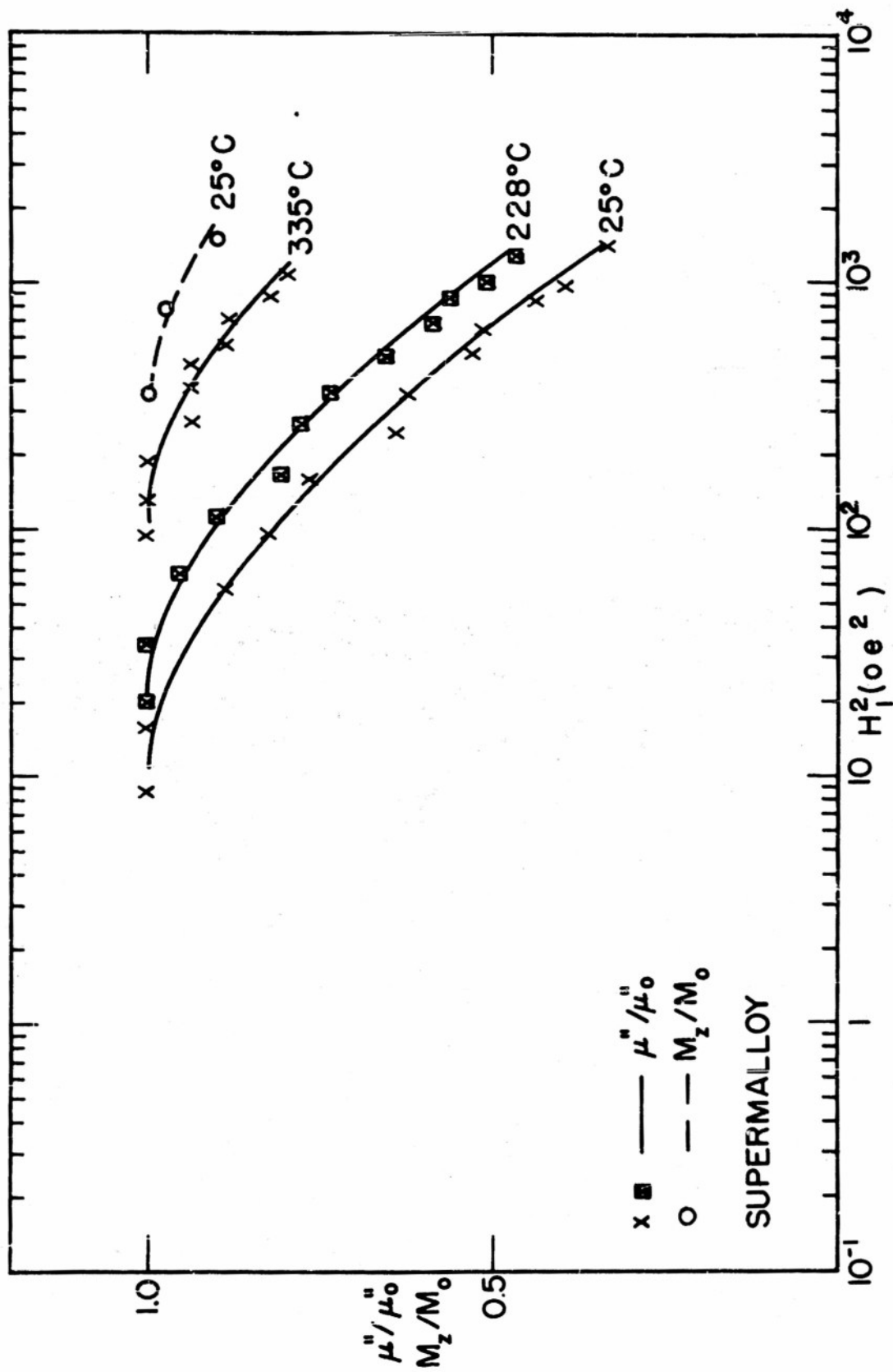


Fig. 16. The value of μ''/μ_0 and M_z/M_0 (dashed curve) in supermalloy as a function of the microwave amplitude. The field H_1 is parallel to the plane of the disk. The curves are qualitatively the same as for ferrites.

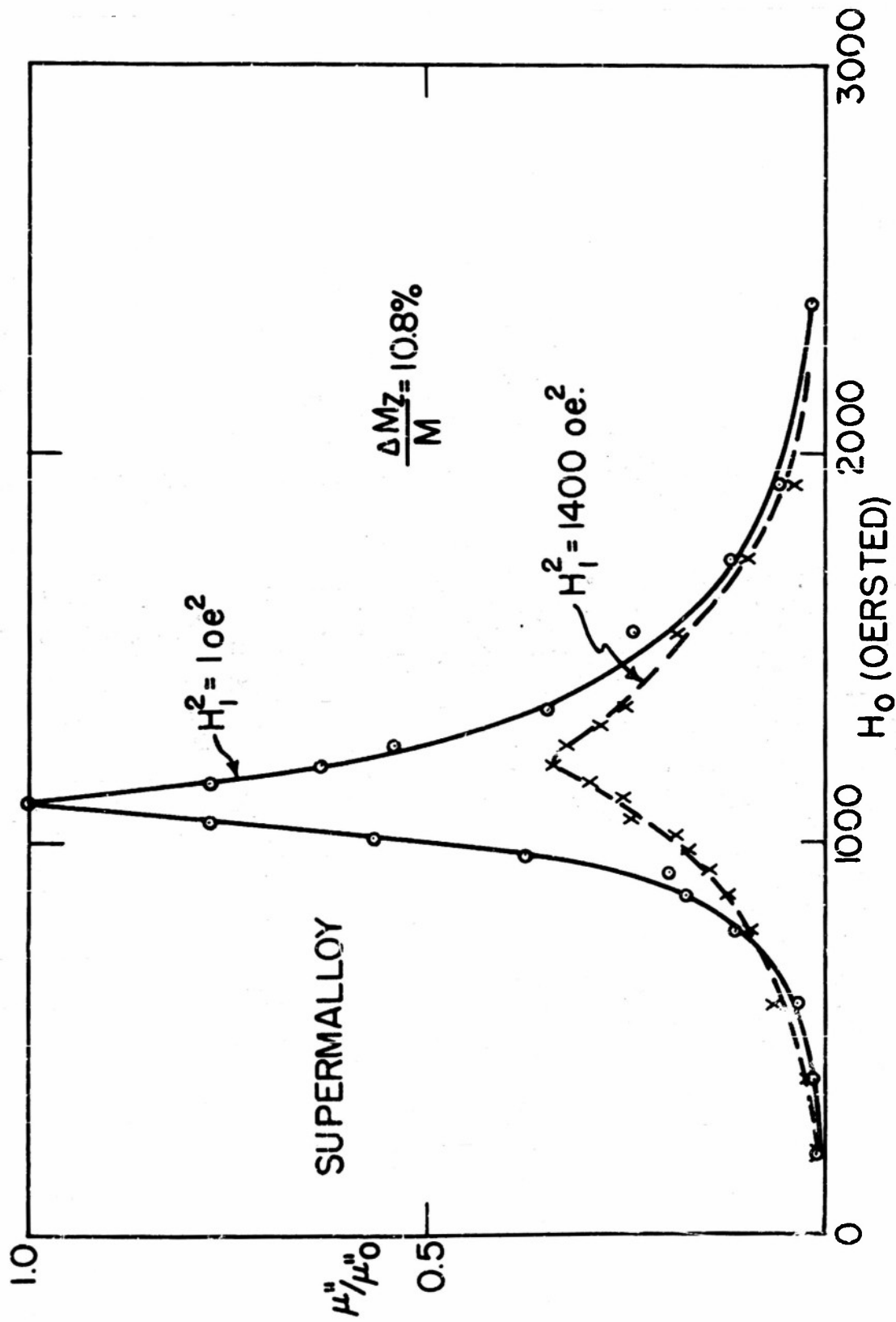


Fig. 17a. The resonance curve for low and high microwave power in a disk of supermalloy with the field H_0 parallel to the plane of the specimen. At 25°C.

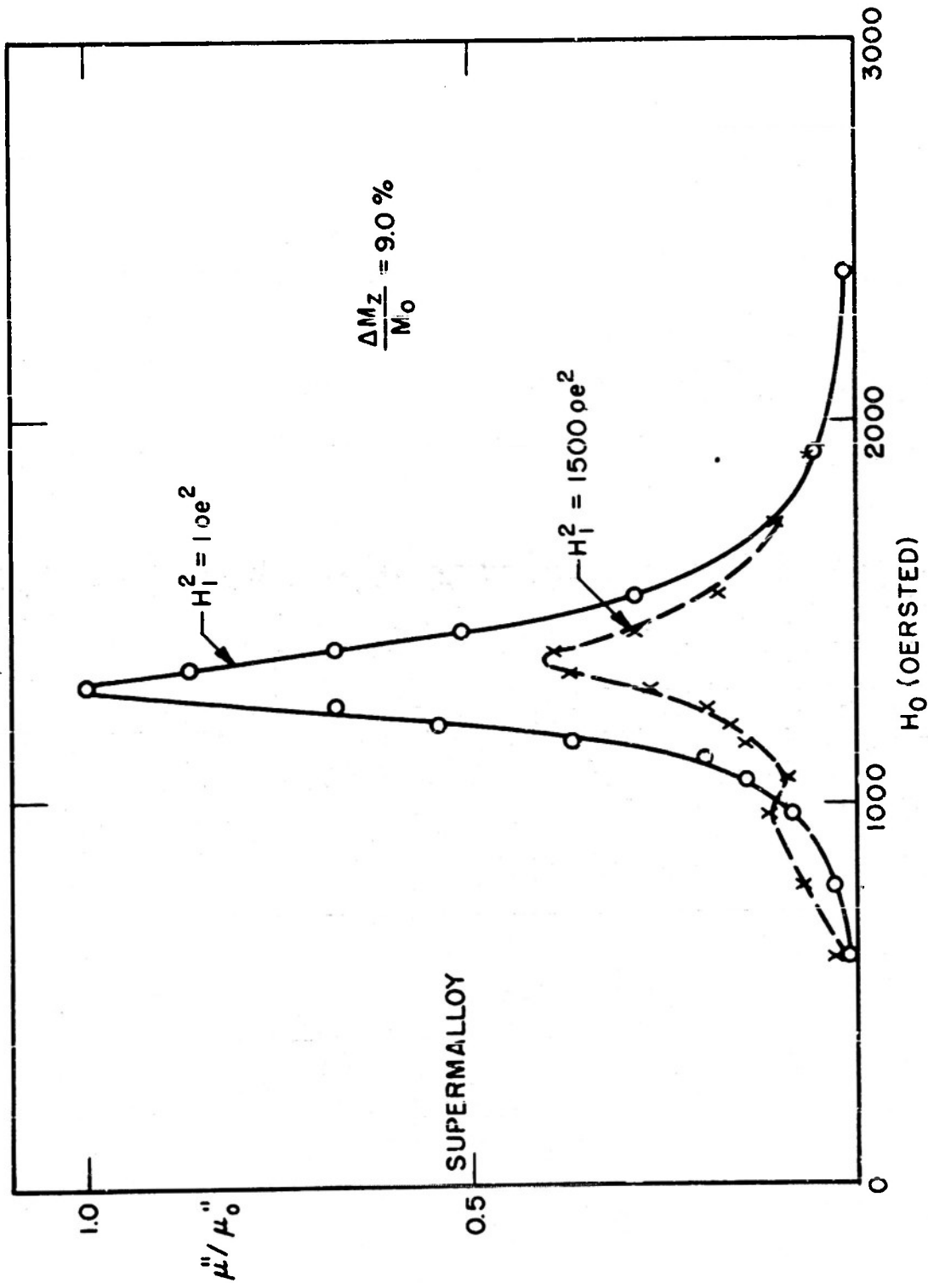


Fig. 17b. The resonance curve for low and high microwave power in a disk of supermalloy with the field H_0 parallel to the plane of the specimen. At 228°C.

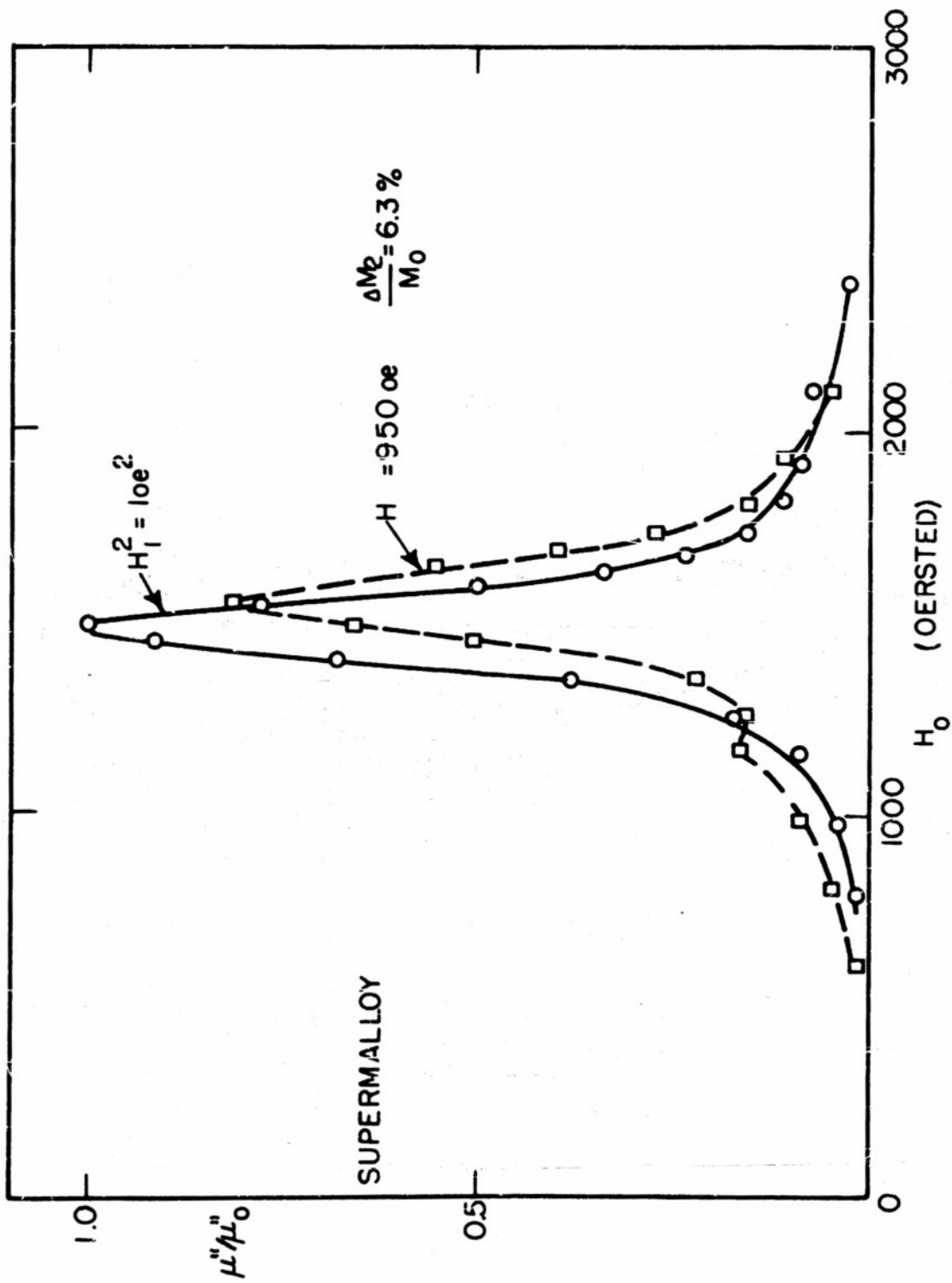


Fig. 17c. The resonance curve for low and high microwave power in a disk of supermalloy with the field H_0 parallel to the plane of the specimen. At 335°C .

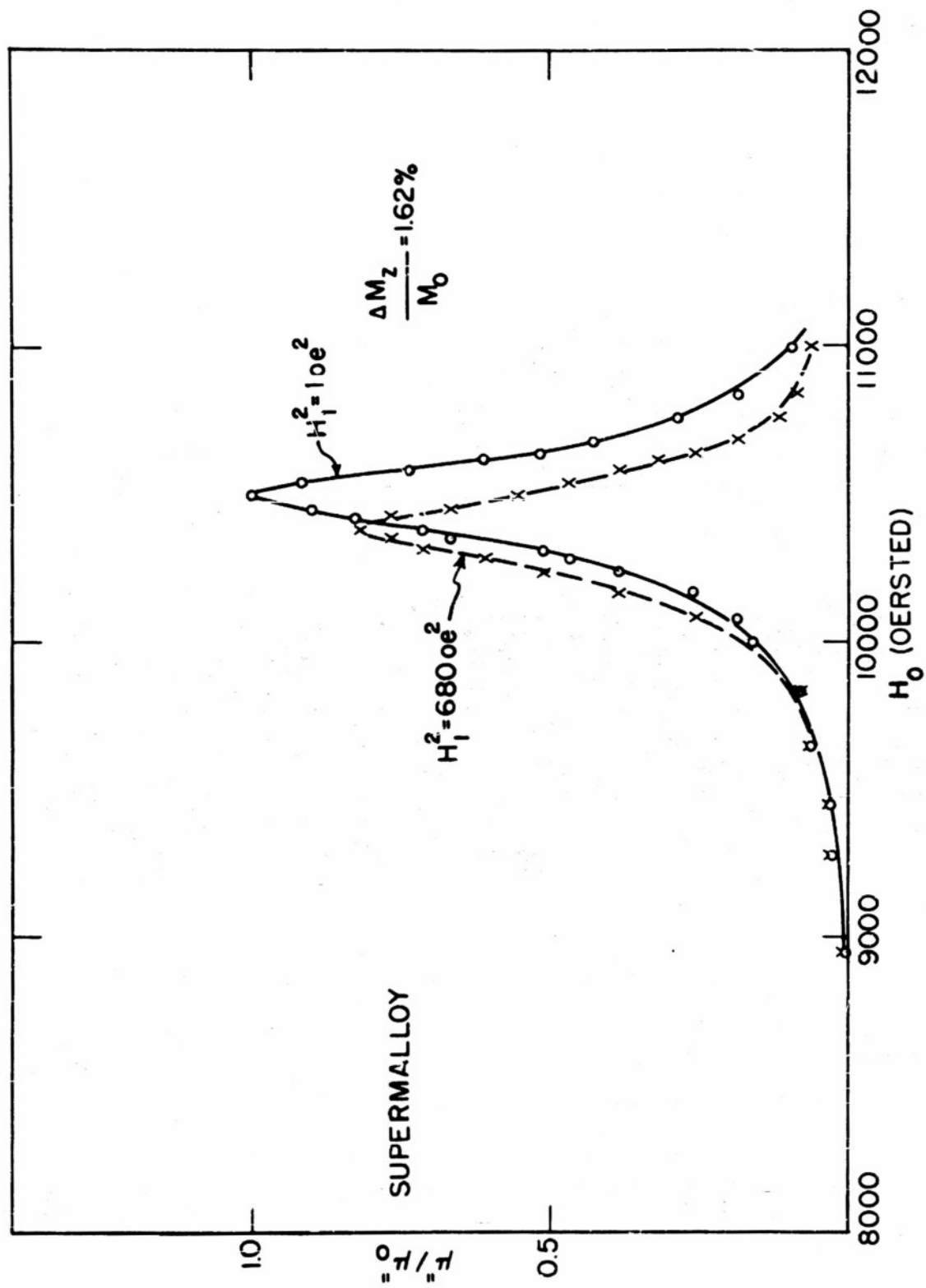


Fig. 18. The resonance curve for low and high microwave power in a disk of supermalloy with the field H_0 perpendicular to the plane of the specimen.

For thermal equilibrium n_k is given by the Bose-Einstein statistical factor

$$n_k = \left(e^{\epsilon_k/kT} - 1 \right)^{-1} \quad (25)$$

The dominant spin-spin relaxation mechanism can be described by the destruction of two spin waves \underline{k} and \underline{l} and the creation of a new one \underline{m} , and the reverse processes. To calculate the probability per unit time for a spin wave k to collide one has to sum over all values of l and m , subject to the conditions of conservation of energy and momentum

$$\epsilon_k + \epsilon_l = \epsilon_m \quad (26)$$

$$\underline{k} + \underline{l} = \underline{m}$$

The net probability for a spin wave in excess of the equilibrium value given by equation (25) to disappear is equal to the inverse of the relaxation time τ_s . Akhieser²⁷ finds

$$\tau_s = \frac{\hbar J}{4 \sqrt{\pi} W^2} \left(\frac{T_c}{T} \right)^{1/2} \ell_n^{-2} \left(\frac{kT}{W} \right) \quad (27)$$

which is an average for all spin waves \underline{k} . The formula is of course restricted to temperatures well below the Curie point T_c . W is the dipolar interaction. In ferromagnetic media one should often not take the classical value $g^2 \beta^2 r^{-3}$, but the pseudo-dipolar interaction C , which may be 10 to 10^2 times larger and may itself depend on temperature.²⁸ The order of magnitude of τ_s between liquid air and room temperature is between 10^{-8} and 10^{-10} sec. The pseudo-dipolar interaction C may increase with decreasing temperature. In this case the relaxation time can become shorter at lower temperatures. This situation seems to occur in nickel zinc ferrite (Figure 11).

Similarly a spin-lattice relaxation time can be calculated by considering collision processes between spin waves and lattice phonons. The lattice vibrations modulate the dipolar interaction between the spin waves. Akhieser,²⁷ Kittel²⁹ and Abrahams³⁰ arrive at a similar conclusion that the spin lattice relaxation for the whole spin system, i. e. an average for

all spin waves, is of the order of 10^{-7} sec.

Polder³¹ pointed out that in ferromagnetic resonance we are not interested in an average for all spin waves but specifically in the very long waves. For collisions with very long waves the restrictions²⁶ imposed by the conservation of energy and momentum are more severe. For $k = 0$ higher order collisions must be considered. Furthermore, the short range pseudo-dipolar interaction is less effective for long waves. The result is that both the spin-spin and the spin-lattice relaxation times at room temperature are increased by factors of the order of 10^5 or 10^6 . They are consequently much longer than the experimental results.

Imperfections or impurities create deviations from perfect periodicity in the spin system. The dipolar interaction then does not have the same form at every lattice point, and the conservation of momentum in k -space can be violated. This would tend to decrease the relaxation time for the long spin waves, but they would then become proportional to the amount of impurity. No such effects have been observed and especially the results for silicon-iron make it necessary to dismiss this suggestion.

The result of Van Vleck³² that the line width tends to zero at low temperatures is in agreement with the picture of colliding spin waves, as was pointed out by Abragam.³³ At absolute zero the interaction with the microwave field $H_1 e^{i\omega t}$ has only matrix elements connecting the ground state with the lowest excited state $n_{k=0} = 1$. If the frequency ω does not exactly correspond to the energy difference $\omega_0 = g\beta H_0/\hbar$, no absorption can take place in first order. By introducing the dipolar interaction we can, however, make a virtual transition to an intermediate state, in which energy is not conserved. Second-order perturbation theory gives for the matrix element to a final state with two spin waves with opposite momenta, since momentum has to be conserved in each step,

$$\frac{(n_{k=0}=0, n_{\ell}=0, n_{-\ell}=0 | H_1 | n_k=1, n_{\ell}=0, n_{-\ell}=0) (n_k=1, n_{\ell}=0, n_{-\ell}=0 | W | n_k=0, n_{\ell}=1, n_{-\ell}=1)}$$

$$\pi(\omega = \omega_0)$$

The frequency at which second-order absorption takes place is given by

$$\hbar\omega = \epsilon_p + \epsilon_{-p}$$

and is therefore at least twice the resonant frequency ω_0 . This absorption will of course give a large contribution to the second and fourth moments, but the line width in the usual sense should be zero.

Keffer³⁴ and Kittel²⁹ conclude, however, that the total second and fourth moments of the line give a real indication of the line width and spin-spin relaxation time even at very low temperatures. They point out that the zero point energy of the spin waves is responsible for transverse components of the magnetization and creates internal fluctuating fields of the same order of magnitude as near the Curie temperature. They then apply the argument of Gorter and Van Vleck¹⁴ for exchange narrowing of these internal zero point fields and obtain essentially the same line width

$$\hbar\Delta\omega = C^2/JS \quad (28)$$

as Anderson and Weiss²⁰ found above the Curie point. While it is physically acceptable in the paramagnetic region to describe the effect of exchange on the dipolar interaction as a random modulation - and this is the essential basis for the theory from which equation (28) is derived - this does not seem justifiable below the Curie point. If we use for one moment the spin wave language in the paramagnetic region, we might say that there are such frequent random collisions between them that a random modulation of the dipolar interaction between them results. At the same time, because the collision frequency is comparable to the proper frequencies of the spin waves, the spin wave language has lost its validity above the Curie point. However, this is not so in the ferromagnetic region. In a first approximation the spin waves are not interrupted and their dipolar interaction is modulated by the proper frequencies of the spin waves. The internal zero point field therefore has quite a different frequency spectrum and, in fact this modulation picture in ferromagnets, if pursued somewhat further, leads to the same results as the theories of Akhieser and Van Vleck. Although we are therefore inclined to adhere to these theories, the experimental fact that the line width is constant at low temperatures then remains a mystery. Even if Kittel's explanation for width is accepted,

his theory could not explain other experimental observations. Our results of Figure 10 show that the inverse width cannot be identified with the spin-spin relaxation time t_{He} in ferromagnetic media. We want to stress the point that the evaluation of t_{He} from the general argument of balance of power is straight forward and excludes shorter values of t_{He} . The inverse proportionality of t_{He} and T is more or less consistent with the collision theory of spin waves. But the magnitude of t_{He} is closer to the average value τ_g of equation (27) than the value derived for long spin waves only. It would be worthwhile to measure t_{He} at still lower temperatures and check whether it continues to rise.

The cause for the combined effects of the magnitude and temperature dependence of t_{He} and the value of the line width at low temperatures remains obscure. The same must be said about the increased absorption in the tails and the secondary maximum at high microwave power levels. The features seem to be quite universal as evidenced by Figures 9 and 14, but are contained in no existing theory.

The present experiments, which were undertaken to clarify some of the issues of ferromagnetic relaxation, have only created new problems in this respect. An important point still seems to be missing in the theory below the Curie temperature. But the situation above the Curie point is now clear. The relation between relaxation effects and exchange narrowing is well established. The spin spin relaxation time t_{He} is about equal to the inverse of the width given by equation (28). All terms of the dipolar interaction contribute to the latter. But only that part of it which does not commute with the magnetization M_z contributes to t_{He} .

The spin lattice relaxation time was shown to escape experimental observation, except perhaps in the case of supermalloy at high temperatures. In this case the width and inverse relaxation time increase near the Curie point which could be explained by a temperature dependent interaction with the conduction electrons. If the short experimental values for t_{He} are accepted, there is no difficulty remaining for the spin-lattice relaxation mechanism. The whole spin system then takes part in transferring energy to the lattice and the characteristic times calculated by Akhiezer and Abrahams are short enough, less than $10^3 t_{He}$, to cause no further problems.

Acknowledgment

The authors are indebted to Professors C. Kittel and J. H. Van Vleck and to Drs. A. Abragam and P. W. Anderson for stimulating discussions.

References

1. C. J. Gorter, Paramagnetic Relaxation, Elsevier Publishing Co., Amsterdam, 1947.
2. N. Bloembergen, E. M. Purcell and R. V. Pound, Phys. Rev. 73, 678 (1948).
3. C. P. Slichter, Thesis, Harvard University (1949).
4. N. Bloembergen and R. W. Damon, Phys. Rev. 85, 699 (1952).
5. R. W. Damon, Rev. Mod. Phys. 25, 239 (1953).
6. D. Polder, Phil. Mag. 40, 99 (1949).
7. L. Hogan, Bell Syst. Tech. J. 31, 1 (1952).
8. J. A. Young, Jr. and E. A. Uehling, Phys. Rev. 90, 990 (1953).
9. B. S. Gourary, Report of the Johns Hopkins University, Applied Physics Laboratory, Silver, Md. (1953).
10. N. Bloembergen, Phys. Rev. 78, 572 (1950).
11. P. W. Selwood, Magnetochemistry, Interscience Publishing Co., New York, 1943.
12. C. H. Townes and Turkevich, Phys. Rev. 77, 148 (1950).
13. C. Hutchisson, J. Chem. Phys. 20, 534 (1952).
14. C. J. Gorter and J. H. Van Vleck, Phys. Rev. 72, 1128 (1947).
15. J. H. Van Vleck, Phys. Rev. 74, 1168 (1948).
16. P. W. Anderson and P. R. Weiss, Rev. Mod. Phys. 25, 269 (1953).
17. F. Keffer, Thesis, University of California (1951).
18. J. H. Van Vleck, J. Chem. Phys. 5, 320 (1937).

19. H. B. G. Casimir and F. K. DuPre, *Physica* 5, 507 (1938).
20. P. W. Anderson, *Phys. Rev.* 88, 1214 (1952).
21. N. F. Mott and H. Jones, *The Theory of the Properties Of Metals And Alloys*, Oxford University Press, 1936.
22. C. Kittel, *Introduction To Solid State Physics*, John Wiley and Sons, New York, 1953.
23. C. Kittel, *Phys. Rev.* 73, 155 (1948).
24. N. Bloembergen, *Phys. Rev.* 78, 572 (1950), equation (8).
25. L. Landau and E. Lifshitz, *Phys. ZS Soviet Union* 8, 153 (1935).
26. F. Dicke, Invited Paper at the Cambridge Meeting of the American Physical Society, January 1953.
27. A. Akhieser, *J. Phys. USSR* 10, 217 (1946).
28. J. H. Van Vleck, *Phys. Rev.* 52, 1180 (1937).
29. C. Kittel and E. Abrahams, *Rev. Mod. Phys.* 25, 233 (1953).
30. E. Abrahams and C. Kittel, *Phys. Rev.* 88, 1200 (1952).
31. D. Polder, *Phil. Mag* 40, 99 (1949).
32. J. H. Van Vleck, *Phys. Rev.* 78, 266 (1950).
33. A. Abragam (private communication).
34. F. Keffer, *Phys. Rev.* 88, 686 (1952).

DISTRIBUTION

2 Office of Naval Research (427)
Navy Department
Washington 25, D. C.

1 Office of Naval Research (460)
Navy Department
Washington 25, D. C.

1 Chief, Bureau of Ordnance (Re4f)
Navy Department
Washington 25, D. C.

2 Chief, Bureau of Ships (910)
Navy Department
Washington 25, D. C.

1 Chief, Bureau of Aeronautics (E1.-51)
Navy Department
Washington 25, D. C.

1 Chief of Naval Operations (Op-413)
Navy Department
Washington 25, D. C.

1 Chief of Naval Operations (Op-20)
Navy Department
Washington 25, D. C.

1 Chief of Naval Operations (Op-32)
Navy Department
Washington 25, D. C.

6 Naval Research Laboratory (2000)
Bellevue, D. C.

1 Naval Research Laboratory (2020)
Bellevue
D. C.

1 Naval Research Laboratory (3480)
Bellevue
D. C.

1 Naval Ordnance Laboratory
White Oak
Maryland

- 1 U. S. Naval Electronics Laboratory
San Diego 52
California
- 1 Naval Air Development Center (AAEL)
Johnsville,
Pennsylvania
- 1 U. S. Navy Underwater Sound Laboratory
New London
Connecticut
- 1 U. S. Navy Office of Naval Research
Branch Office
150 Causeway Street
Boston 14, Massachusetts
- 1 U. S. Navy Office of Naval Research
Branch Office
346 Broadway
New York 13, N. Y.
- 1 U. S. Navy Office of Naval Research
Branch Office
The John Crerar Library Building
86 E. Randolph Street
Chicago 1, Illinois
- 1 U. S. Navy Office of Naval Research
Branch Office
801 Donahue Street
San Francisco 24, California
- 1 U. S. Navy Office of Naval Research
Branch Office
1030 Greene Street
Pasadena 1, California
- 2 U. S. Navy Office of Naval Research
U. S. Navy No. 100, Fleet Post Office
New York, N. Y.
- 1 Librarian
U. S. Naval Post Graduate School
Electronics Department
Monterey, California
- 1 U. S. Coast Guard(EEE)
1300 "E" Street, N. W.
Washington, D. C.

- 1 **Research and Development Board**
Pentagon Building
Washington 25, D. C.
- 1 **Dr. N. Smith**
National Bureau of Standards
Department of Commerce
Washington, D. C.
- 1 **Applied Physics Laboratory**
Johns Hopkins University
8621 Georgia Avenue
Silver Spring, Maryland
- 7 **Library of Congress**
Navy Research Section
Washington 25, D. C.
- 1 **Dr. A. G. Hill**
Project Lincoln
Massachusetts Institute of Technology
Cambridge 39, Massachusetts
- 1 **Professor K. Spangenberg**
Stanford University
Stanford, California
- 1 **Professor E. C. Jordan**
University of Illinois
Urbana, Illinois
- 1 **Dr. V. H. Rumsey**
Ohio State University
Columbus, Ohio
- 1 **Dr. C. R. Burrows**
Department of Electrical Engineering
Cornell University
Ithaca, New York
- 1 **Electrical Engineering Department**
University of California
Berkeley, California
- 1 **Professor J. J. Brady**
Oregon State College
Corvallis, Oregon
- 1 **Electrical Engineering Department**
University of Texas
Box F, University Station
Austin, Texas

- 1 Library
Philco Corporation
Philadelphia 34, Pennsylvania
- 1 Technical Library
Bell Telephone Laboratories, Inc.
Murray Hill, New Jersey
- 2 Librarian
National Bureau of Standards
Washington 25, D. C.
- 1 Librarian
Radio Corporation of America
RCA Laboratories Division
Princeton, New Jersey
- 1 Exchange Section, American and British
Exchange and Gift Division
Library of Congress
Washington 25, D. C.
- 1 Professor Morris Kline
Mathematics Research Group
New York University
45 Astor Place
New York, N. Y.
- 1 Technical Library
Federal Telecommunications
500 Washington Avenue
Nutley 10, New Jersey
- 1 Librarian
Central Radio Propagation Laboratory
National Bureau of Standards
Washington 25, D. C.
- 1 Mr. R. E. Campbell
Room 22-B-104
Massachusetts Institute of Technology
Cambridge 39, Massachusetts
- 1 Watson Laboratories Library, AMC
Red Bank
New Jersey
(ENAGS1)
- 1 Mr. J. Hewitt, Document Room
Research Laboratory of Electronics
Massachusetts Institute of Technology
Cambridge 39, Massachusetts

- 1 Dr. John V. N. Granger
Stanford Research Institute
Stanford, California
- 1 Radiation Laboratory
Johns Hopkins University
1315 St. Paul Street
Baltimore 2, Maryland
- 1 Mr. R. Damon
The Knolls
General Electric Company
Schenectady, N. Y.
- 1 Mrs. Mary Timmins, Librarian
Radio and Television Library
Sylvania Electric Products
70 Forsythe Street
Boston 15, Massachusetts
- 1 Library of the College of Engineering
University Heights Library
University Heights 53, New York
- 1 Documents and Research Information Center
Raytheon Manufacturing Company
Equipment Engineering Division
Newton, Massachusetts
- i Professor W. B. Davenport, Jr.
Lincoln Laboratory
Massachusetts Institute of Technology
Lexington, Massachusetts
- 50 Dr. H. A. Zahl
Transportation Officer
Second Avenue and Langford Street
Asbury Park, New Jersey
Contract N5ori-76, T. O. I.
- 50 Chief, Administration Section
Division Services Branch
Electronics Research Division
Air Force Cambridge Research Center
230 Albany Street
Cambridge 39, Massachusetts